REVISION OF THE *DIPODOMYS MERRIAMI* COMPLEX IN THE BAJA CALIFORNIA PENINSULA, MEXICO

Sergio Ticul Álvarez-Castañeda,* William Z. Lidicker, Jr., and Evelyn Rios

Centro de Investigaciones Biológicas del Noroeste, S.C., Mar Bermejo 195, A.P. 128, La Paz, Baja California Sur, 23090, México (STÁ-C, ER)
Museum of Vertebrate Zoology and Department of Integrative Biology, University of California, Berkeley, CA 94720, USA (WZL)

The kangaroo rat *Dipodomys merriami* occurs widely over the Baja California peninsula, inhabiting all the arid and sandy lowlands. Its range encompasses diverse climatic, edaphic, and vegetation zones, including 2 islands. The 11 taxa recognized in the *merriami* complex in this region almost 50 years ago remain valid to the present. The 2 island forms originally were described as different species, and have been treated in different ways by subsequent authors. In this investigation we used a genetic analysis of 2 mitochondrial genes, cytochrome *b* (*Cytb*) and cytochrome *c* oxidase subunit III (*COIII*), to study patterns of genetic structuring in this species throughout the peninsula. We supplemented existing morphometric and pelage color data with new data, and integrated these data sets into a phylogenetic analysis. Finally, we explored how our results compared with the existing taxonomic arrangement of species and subspecies. Our phylogenetic analyses of molecular data used the concatenation of 1,140 base pairs (bp) of the *Cytb* gene and 690 bp of the *COIII* gene; cladograms were generated using maximum-parsimony, maximum-likelihood, and Bayesian inference procedures. A hierarchy of nested clades was produced, the highest level of which revealed 2 reciprocally monophyletic clades separated by 20 mutational steps. There is a Southern Clade extending north to the Vizcaíno Desert in the west and San José Island in the east, and a Northern Clade that includes all the populations farther to the north. At a shallower level, the Southern Clade contains 4 subclades, including the populations of San José and Margarita islands, whereas the Northern Clade is composed of 3 subclades. Adding the morphometric and pelage coloration data sets to the analyses resulted in support for the 11 previously recognized taxa arranged in a single species, *Dipodomys merriami*, but with improved understanding of how the subspecies relate to each other. As is increasingly appreciated, our investigation supports a comprehensive approach involving multiple data sets that are sensitive to a wide temporal range of evolutionary history for phylogenetic reconstruction.

Key words: kangaroo rat, mitochondrial DNA, multiple data sets, nested clade phylogeographic analysis, phylogenetics, subspecies, taxonomy

As part of a continuing program of research on the phylogenetic relationships and evolutionary history of mammals occurring in the partially isolated and physiographically complex Baja California peninsula, we investigated the taxonomic status of the *Dipodomys merriami* complex of kangaroo rats inhabiting this region. We employed modern molecular and phylogenetic techniques to evaluate this complex of taxa that exhibits various levels of differentiation and includes populations of conservation concern. In spite of the potential importance of these multiple objectives, the *D.*

merriami complex has not been comprehensively analyzed for 50 years (Lidicker 1960). To do this we used mitochondrial DNA (mtDNA; cytochrome *b* [Cytb] and cytochrome *c* oxidase subunit III [*COIII*]) genes as neutral markers to attempt to resolve the phylogenetic relationships within the complex. Morphometric features and pelage coloration were used to study the pattern of geographic differentiation that is likely related to selective pressures for adaptation to varying degrees of aridity as expressed by precipitation, soil type and color, and vegetation structure. Overall, our goal was to recognize phylogenetically significant units based on the extent to which they show independent evolutionary trajectories (Lidicker 1960, 1962) and to estimate the relative timing of those events. To identify such units, we searched for evidence of reduced gene flow between presumptive evolutionary units coupled with phenotypic coherence within them.

* Correspondent: sticul@cibnor.mx

Our results should lead to an improved understanding of the factors that have generated the phylogenetic history of this group of kangaroo rats.

Currently, the *D. merriami* complex is considered to include 3 species in Baja California, *D. merriami* on the mainland and 2 island forms, *D. insularis* and *D. margaritae* (Alexander and Riddle 2005; Espinoza-Gayosso and Álvarez-Castañeda 2006). *D. merriami* on the mainland is arranged into 9 subspecies within the peninsula (Lidicker 1960). *D. insularis* occurs only on Isla San José off the east coast (Sea of Cortez), and *D. margaritae* is restricted to Isla Margarita off the west coast (Merriam 1907). The development of novel molecular genetics techniques and tools for data analysis and phylogenetic reconstruction provide the methodologies for investigating the systematics of this group of kangaroo rats (Patton and Álvarez-Castañeda 1999). Previous investigations into the *merriami* complex in Baja California have suggested that a major genetic break occurs across the middle of the peninsula with likely taxonomic implications (Alexander and Riddle 2005; Riddle et al. 2000).

The 2 island populations have been particularly controversial as to their taxonomic status. Interest has been generated because of conservation concerns, as well as the general attraction of islands as windows into evolutionary processes. Originally, Merriam (1907) described these 2 island forms as full species. In a revision of the entire *D. merriami* species complex, however, Lidicker (1960) concluded that, on morphological grounds, *D. margaritae* should be considered a subspecies of *merriami*. *D. insularis*, in contrast, was morphologically quite distinct and had features suggesting that it was the least specialized for arid conditions (that is, most primitive in this respect) of any extant population over the entire range of the species complex. Later, Best and Janecek (1992) published a statistical analysis of somatic and craniodental measurements demonstrating that the 2 island forms were significantly different from mainland populations, and also differed in bacular features. However, they found few differences in allozyme characters, and concluded that overall subspecific status was appropriate. Two subsequent reviews of this situation (Patton and Álvarez-Castañeda 1999; Williams et al. 1993) maintained this subspecies arrangement. Others have returned to the original species status for these island endemics (Best 1992; Best and Thomas 1991; Hall 1981). Finally, a study of the entire family Heteromyidae using mtDNA sequence data (Alexander and Riddle 2005) showed that populations from the islands of San José and Margarita are in the same clade as adjacent mainland populations with very low divergences. Nevertheless, they maintained the species-level designation for the 2 island taxa. Patton (2005) treat them at the subspecific level.

MATERIALS AND METHODS

Sample collection.—A total of 510 museum specimens from throughout the Baja California peninsula was used in the morphological analyses (see Appendix I for allocation of specimens to databases). This series includes a large number of specimens reported in Lidicker (1960) for which original measurements were incorporated. Specimens were grouped into 18 physiographic regions based on the arrangements of Cuanalo et al. (1989; see Fig. 1). All of the new material is deposited in the Centro de Investigaciones Biológicas del Noroeste. Specimens were captured and handled following protocols approved by the Animal Care and Use Committee of the American Society of Mammalogists (Gannon et al. 2007).

For the genetic analyses we used 2 different genes, *Cytb* and *COIII*. A total of 126 specimens were sequenced, and they were from localities across the range of the species in Baja California. All 18 physiographic regions were represented, including the 2 island forms, except for physiographic regions 5 (San Quintín) and 6 (Santa Catarina), from which tissue samples were not available.

Laboratory procedures.—Genomic DNA was extracted in the laboratory from liver tissues originally preserved in 95% ethanol using the DNeasy Kit (QIAGEN, Inc., Valencia, California). Initially, a fragment of the *Cytb* gene (~800 base pairs [bp]) was amplified for all 126 samples using the primer pairs MVZ05 (CGA AGC TTG ATA TGA AAA ACC ATC GTT)/MVZ16 (AAA TAG GAA RTA TCA YTC TGG TTT RAT), or MVZ05/spermo 06 (TAT GGG TGA AAG GGR AYT TTA TCT). Later, a subset of 22 samples from representative localities was amplified for the complete *Cytb* gene (1,140 bp), using primers MVZ127 (TRY TAC CAT GAG GAC AAA TAT C)/MVZ 14 (GGT CTT CAT CTY HGG YTT ACA AGA) and MVZ45 (ACM ACH ATA GCM ACA GCA TTC GTA GG)/MVZ14. Additionally, a 690-bp fragment of the *COIII* gene was amplified for these 22 samples using primers L8618 (CAT GAT AAC ACA TAA TGA CCC ACC AA) and H9323 (ACT ACG TCT ACG AAA TGT CAG TAT CA—Riddle 1995).

The following conditions for initial double-stranded amplifications were used: 12.5 µl of template (10 ng), 4.4 µl of double-distilled H$_2$O, 2.5 µl of each primer pair (10 nM concentration), 0.474 µl (0.4 nM) of deoxynucleoside triphosphates, 0.5 µl (3 mM) of MgCl$_2$, 0.125 µl of Taq polymerase (platinum, Invitrogen, Carlsbad, California), and 1× Taq buffer to a final volume of 25 µl. Amplification conditions consisted of 3 min initial denaturation at 94°C followed by 37 cycles of denaturation at 94°C for 45 s, 1 min annealing at 50°C, and 1 min extension at 72°C. Amplified products were purified using the QIAquick PCR Purification Kit (QIAGEN). The templates were cycle-sequenced with MVZ05/MVZ16, MVZ127/MVZ14, and MVZ45/MVZ14 for *Cytb* amplifications, and L8618/H9323 for *COIII* using Big Dye terminator chemistry (Applied Biosystems Inc., Foster City, California), and were run on an ABI 377 automated sequencer (Applied Biosystems Inc.) following manufacturer protocols. MVZ16, MVZ14, and H9323 were used to sequence the reverse strand in 10 individuals in order to check for accuracy. Representative haplotypes generated for this study have been deposited in GenBank (accession numbers EU660963–EU661071 and EU667412–EU667417).
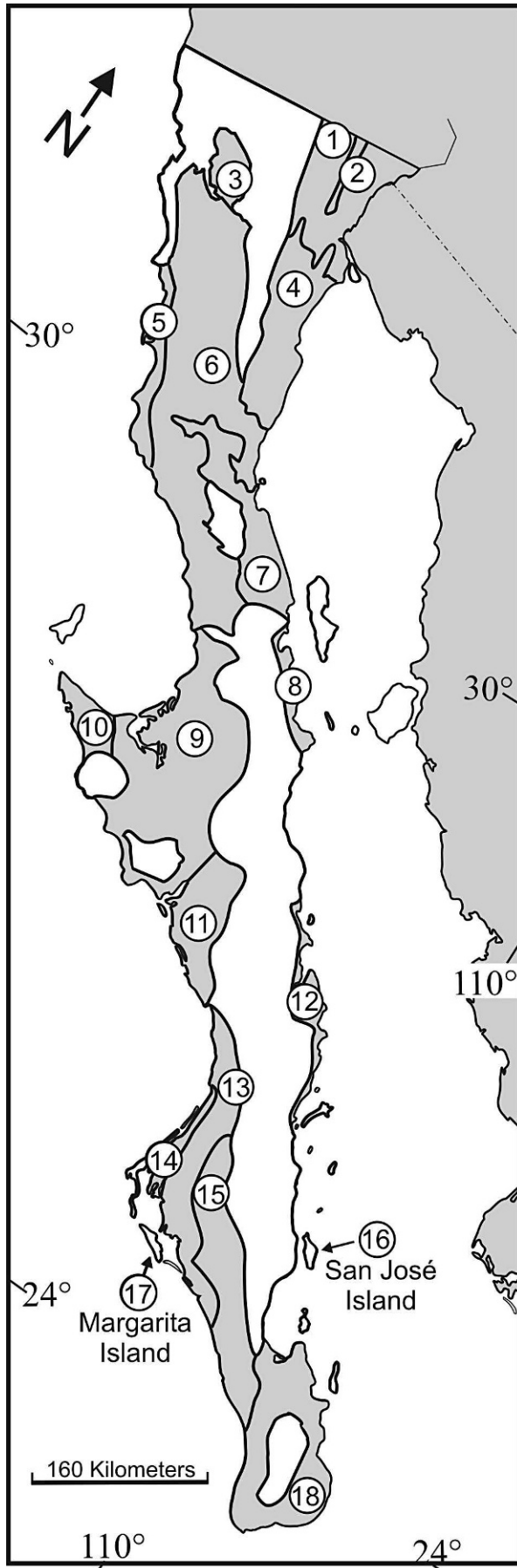
Sequence alignment and haplotype determination.—Nucleotide sequences were aligned using Sequencher version 3.1 software (Gene Codes Corp., Ann Arbor, Michigan), checked by eye, and translated into amino acids for confirmation of alignment. Initially, we obtained sequences for a 500-bp fragment of *Cytb* for all 126 samples and TCS version 1.18 program (Clement et al. 2000) was used to identify 81 unique haplotypes. From these haplotypes, we selected samples that had 22 unique haplotypes that corresponded to representative specimens of the physiographical areas in which the species occurs. In order to increase the number of characters available for analysis, we sequenced the complete *Cytb* gene (1,140 bp) and a 690-bp fragment of the *COIII* gene for these 22 samples.

Two separate analyses were conducted. First, a nested clade phylogeographic analysis was performed based on the 500-bp fragment of *Cytb* from 126 specimens. Second, a phylogenetic analysis was performed. Initially we analyzed the sequence data for the 2 genes separately, and found a general concordance between them. They both revealed the major lineages identified by the nested clade analysis. We then concatenated the data for the 22 representative specimens (1,140 bp of *Cytb* and 690 bp of the *COIII* gene). Voucher specimens are deposited in the Centro de Investigaciones Biológicas del Noroeste (CIB). In order to estimate the haplotypic and nucleotide variation within the physiogeographical groups, we used Arlequin version 2.001 (Schneider et al. 2000).

Nested clade phylogeographic analysis (NCPA).—A nested clade phylogeographic analysis using haplotypes derived from the 500-bp fragment of the *Cytb* and the ANeCA version 1.1 software (Panchal 2007) was undertaken to determine the relative contribution of historical versus contemporary evolutionary processes to the geographical patterns of mtDNA variation. This program automates the nesting algorithm, publishes inference keys, and links together the various components (Panchal 2007; Panchal and Beaumont 2007). ANeCA uses the TCS version 1.18 program (Clement et al. 2000) to construct networks using the algorithm of Templeton et al. (1992). For the nested design of haplotypes in clades, ANeCA follows Templeton et al. (1987) and Templeton and Sing (1993) to define an evolutionary clade hierarchy within the intraspecific haplotype network. It then uses the GeoDis

←

FIG. 1.—Map of the Baja California peninsula indicating the location of the 18 physiographic areas used for the analyses (Cuanalo et al. 1989). The names of these provinces were modified to reflect geographical characteristics of each region or previous names used (Álvarez-Castañeda et al. 1995). The specific collection localities for each area are presented in Appendix I. The light area represents mountains and others areas in which *Dipodomys merriami* is not present. The regions used for this analyses are: 1) Mexicali, 2) Laguna Salada, 3) Valle de la Trinidad, 4) San Felipe, 5) San Quintin, 6) Santa Catarina, 7) Cataviña, 8) Bahía de los Ángeles, 9) Vizcaíno Desert, 10) Bahía Tortugas, 11) San Juanico, 12) Santa Rosalía, 13) Hiray Plains, 14) Pacific Coast, 15) Magdalena Plains, 16) San Jose Island, 17) Margarita Island, and 18) Cape Region.

version 2.2 (Posada et al. 2000) software to define the clades that showed both genotypic and geographic variation. In order to test for patterns of isolation by distance, the nested haplotype structures were correlated with respect to the geographic distance between sampling sites.

Under the ''island forms as separate species'' hypothesis and using only our molecular data, there should be no significant positive correlation between haplotype differences and geographical distances, because these samples would represent populations long-isolated from each other. By contrast, if the 2 populations are at the subspecific level of differentiation, the correlations would ordinarily be positive because nearby populations would be relatively little differentiated from the island forms by mitochondrial haplotype features. The nested clade analysis would then fail to reject the null hypothesis that increased haplotype differentiation was consistently correlated with geographic distance between the populations. However, taxonomic conclusions based on these important insights from nested clade analysis must be tempered by evidence for differentiation of potentially strongly selected morphological, behavioral, or other traits, especially where there is a demonstrable lack of gene flow between populations being compared, such as with islands. There are certainly many examples in the literature documenting species-level differentiation over relatively short time spans.

An analysis of molecular variance (AMOVA) among the nested clades was conducted using the 126 sequences derived from the shorter *Cytb* fragment (500 bp), and analyzed using the program Arlequin version 2.001 (Schneider et al. 2000). Statistical significance ($P < 0.05$) was determined according to the TCS version 1.20 program (Clement et al. 2000) utilizing the algorithm of Templeton et al. (1992). To avoid confusion in terminology between the nested clade and the phylogenetic analyses, we use the name ''nested clade'' for the results of the former and ''clades'' for the latter.

Phylogenetic analyses.—The General Time Reversible model with a fraction of invariable sites and gamma-distributed among-site rate variation (GTR + I + G—Tavaré 1986) was shown to be the most appropriate model for this data set using the model comparison software MrModeltest version 2 (Nylander 2004) under the Akaike information criterion for the concatenated complete *Cytb* and *COIII* fragments. A Bayesian analysis was performed using MrBayes version 3.1.1 software (Ronquist and Huelsenbeck 2003). Four separate runs were performed with Markov chain Monte Carlo simulations starting from a random tree. Each run was conducted with 5,000,000 generations and sampled at intervals of 1,000 generations. The first 5,000 samples of each run were discarded as burn-in and all the remaining sampled trees were analyzed to find the posterior probability of clades. A consensus tree was generated with the 50% majority-rule algorithm in PAUP* 4.0b10 (Swofford 2000), and the percentage of samples recovered in a particular clade was assumed to be the posterior probability of that clade.

Genetic distances were calculated using the GTR + I + G model and the Kimura 2-parameter model. The latter is the most

commonly used model for comparing levels of divergence among studies (Baker and Bradley 2006). A neighbor-joining analysis was conducted in PAUP* 4.0b10 (Swofford 2000). Support for nodes was assessed with bootstrap analyses, including a fast heuristic procedure with 1,000 pseudoreplicates. Sequences from Alexander and Riddle (2005) were downloaded from GenBank and were included in the analyses for *Dipodomys insularis* (*Cytb* = AY926371, *COIII* = AY926438), *D. margaritae* (*Cytb* = AY926370, *COIII* = AY926437), *D. merriami* (*Cytb* = AY926383, *COIII* = AY926450), *D. simulans* (*Cytb* = AY926367, *COIII* = AY926434), *D. venustus* (*Cytb* = AY926373, *COIII* = AY926440), *D. elephantinus* (= *D. venustus elephantinus*) (*Cytb* = AY926374, *COIII* = AY926441), and *D. phillipsii* (*Cytb* = AY926376, *COIII* = AY926443). The outgroup specimens were chosen following Alexander and Riddle (2005).

Maximum-parsimony and maximum-likelihood analyses were implemented in PAUP* 4.0b10 (Swofford 2000). For maximum-parsimony analysis, all characters were equally weighted, and heuristic searches were performed with 1,000 random additions of sequences and a tree-bisection-reconnection algorithm was used for branch swapping. For all analyses that resulted in multiple most-parsimonious trees, consensus trees were constructed using the 50% majority rule. The GTR + I + G model was then used for maximum-likelihood searches consisting of 100 random replicates with tree-bisection-reconnection branch swapping. Bootstrap values ≥50% are reported for branch support.

Morphological analysis.—For the present study, we used the same characters that were measured by Lidicker (1960) in his earlier revision of *D. merriami*, except that we restricted our analysis to the Baja California peninsula. For some populations, however, the number of specimens that were measured had to be increased in order to improve the statistical analyses. Only adult specimens ($n = 510$) were included in the analysis (Appendix I). Nine linear characters were measured from cleaned skulls using dial calipers (0.01-mm resolution). The characters measured were: basal length of skull (BLS), total cranial length (CL), nasal length (NL), maxillary breadth (MxB), least interorbital breadth (IB), greatest cranial breadth (CB), rostral width (RW), alveolar length of maxillary toothrow (ALMx), and the least width of supraoccipital (WS). See Lidicker (1960) for details. Adults were defined as having complete adult dentition with all teeth showing some wear, and the auditory bullae revealing some translucence. Most cranial and body measurements exhibited sexual dimorphism, with males being larger, but the differences were slight for most traits. For this reason and because specimen samples did not show any systematic sex ratio bias, sexes were combined for these analyses.

Geographic variation.—An analysis of variance (ANOVA) for each of the 9 craniodental measurements was performed (Statistica version 5.0, Starsoft, Inc., Tulsa, Oklahoma) among all the physiographical areas; geographical areas in close proximity were subsequently compared with Tukey's honestly significant difference using the unequal *N* (Spjotvoll/stoline)

test. We also performed a discriminant function analysis to distinguish between specimens of adjacent physiographical regions using all of the craniodental characters.

To search for possible geographic variation in the relationships among cranial morphology, we used principal component analyses that included all cranial measurements (Statistica version 5.0). Collecting localities were grouped according to the 18 physiographic regions following Cuanalo et al. (1989), and were plotted on the first 3 principal components (PCs). Residuals obtained from the regression of each original craniodental variable on PC-I and PC-II scores were used to conduct ANOVAs and a posteriori Tukey's honestly significant difference utilizing the unequal N (Spjotvoll/stoline) test to evaluate size and shape differences between groups of collecting localities.

Pelage color analysis.—Pelage color of 373 adult specimens was determined employing an X-Rite Digital Swatchbook spectrophotometer (X-Rite, Inc., Grandville, Michigan). The instrument provided a reflectance spectrum (390–700 nm) of the object being measured as well as tri-stimulus color scores (red, green, and blue wavelengths). Individuals in molt were excluded. Color was measured with a 3-mm-diameter port placed on 2 topographic positions on each individual specimen: on the rump, and on the middorsal stripe of the tail, in the penicillate part. Three replicas of each color score were assessed at each position and averaged. The hue and chroma of each area were recorded using Munsell Soil Color Charts (Munsell Color Co. 1975).

The variation in brightness was obtained by adding the values of the 3 color parameters on the assumption that higher color intensities translate into brightness. An ANOVA was performed to determine differences in brightness among individuals (Patton et al. 2007) from different physiographical regions. If brightness is represented by the sum of the intensities of the 3 colors, it is possible that pelages might be very different in color (chroma) even with the same brightness. However, in our samples all populations are similar chromatically on the rump and dorsal caudal stripe so we think the brightness indices are comparable, and therefore meaningful.

Results

Nested clade phylogeographic analysis.—To construct the network we used the data set based on a 500-bp fragment of *Cytb* from 126 specimens, with 81 unique haplotypes (Table 1 and Appendix II). We found that the maximum number of mutational steps between haplotypes allowing parsimonious connections was 9 steps ($P \geq 0.95$). Using maximum parsimony within these limits, 4 disjointed networks were obtained: Northern (not shown), Coastal, Central, and Southern networks. The Southern network, corresponding to the Southern Clade of the phylogenetic analysis, was separated from the other 3 by a minimum of 11, 14, and 20 mutational steps, respectively (Fig. 2), well beyond the confidence limits for parsimony. Because an important objective of this study

was to examine the taxonomic status of island forms in the south of the peninsula, we analyzed the relationships within this network. In the southern peninsula sample, the inference key of the nested clade analysis showed that the null hypothesis of random geographical association cannot be rejected, for all clades within a nesting category, except for clade 2-7, which revealed a contiguous range expansion. The only nested clade with a significant relationship ($P = 0.03$) was 3-2 (San Jose Island). However, the internal tip (*I-T*) status was undetermined because the outcome was inconclusive.

The Southern nested clade mainly included all the haplotypes present south of San Ignacio Lagoon. The nested clade analysis suggested the presence of 4 geographical groups. Two of these were the island subclades (1-2 and 1-8), and there was not statistical support to consider them different from those of the mainland. A 3rd geographical group occurred in the area extending from the northern part of La Paz to the southern part of physiographic region 14 (subclades 2-1, 2-4, 2-7, 2-8, and 2-10). A 4th geographical group extended from the La Paz isthmus (region 18) to the south (subclades 2-3, 2-12, and 2-13).

The 3 nested networks from north of the San Ignacio Lagoon (Northern, Central, and Coastal) provided less information on genetic substructure. The Central network with 4 nested clades showed restricted gene flow with isolation by distance in clades 3-1 and 3-2. The areas inhabited by clade 3-1 included the western lowlands of the Vizcaíno Desert and southwest of the Central Desert. This area is characterized by very sandy soils and even some sand dunes. Clade 3-2 occurred on the Vizcaíno Desert slopes along the west side of the Sierra de la Giganta. However, none of the 4 nested clades in this network showed significant differences ($P < 0.05$) among them.

The Coastal network was split into 2 statistically significant ($P < 0.05$) areas, revealing an allopatric fragmentation. There was a northern geographical area (3-1) comprised of subclades Bahía de los Ángeles (2-1) and southern Bahía de los Ángeles (2-4). A southern geographical area (3-2) was similarly divided into 2 subclades: Mulegé (1-4) and La Purísma (1-3).

Statistical analysis (AMOVA) of *Cytb* (500 bp) using all 4 networks in the total cladogram (NCPA) showed (Fig. 2) a variation of -2.29% among groups (these negative variance components indicate an absence of genetic structure—Schneider et al. 2000), 5.73% among populations within groups, and 94.56% within populations. In the vicinity of San Juanico (CIB 7323, 7324, region 11), haplotypes of both the Southern and Central networks were found. Taken as a whole, the total cladogram (*I-T*) provided no statistical support for any particular arrangement of inclusive clades.

Phylogenetic analysis.—The maximum-parsimony analysis of the molecular data of the concatenated *Cytb* and *COIII* genes yielded 1 tree (length = 751, consistency index = 0.752, retention index = 0.880). The GTR + I + G was the best-fit model of nucleotide substitution (A = 0.298, C = 0.285, G = 0.130, and T = 0.285, invariable sites = 0.465, and gamma distribution = 0.763).
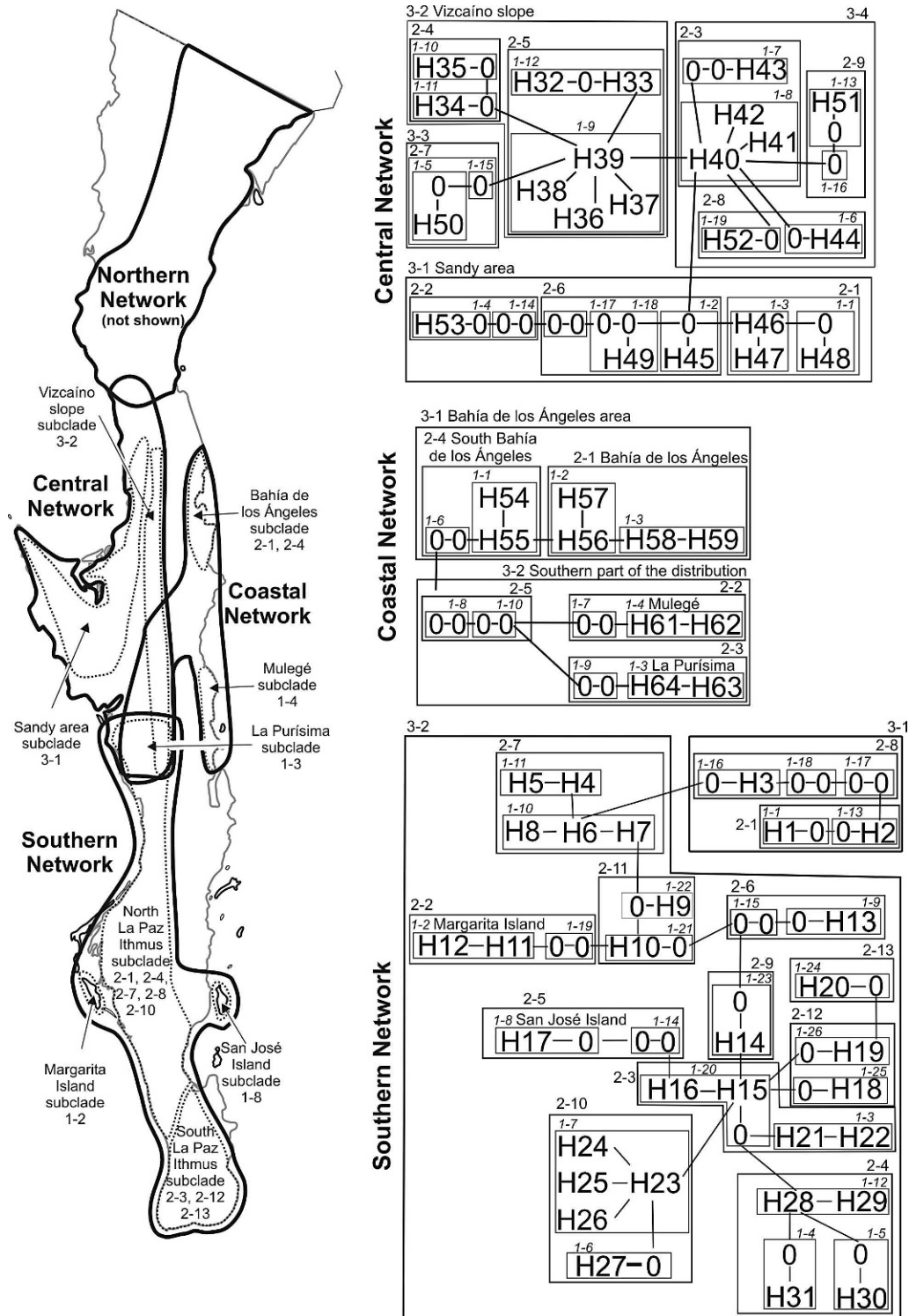
FIG. 2.—The nested design inferred for the 4 networks constructed from the 81 haplotypes for the cytochrome *b* (*Cytb*) gene (500 bp) found on the peninsula. The left side shows the geographic projection of networks and subclades displayed graphically on the right side. In each network, hypothetical haplotypes are represented by 0. Thin-lined polygons enclose numbered (*n*) 1-step clades and are designated by 1-*n*; medium-lined polygons enclose numbered 2-step clades (2-*n*); thick-lined polygons enclose 3-step clades (3-*n*). The northern network is not shown as no significant genetic variation was found within it.

Bayesian inference (4 replicates) converged on essentially identical tree topologies. This result showed 2 monophyletic clades: 1 represented the samples from the southern part of the peninsula, including Margarita and San José islands, and the 2nd represented all of the northern populations plus physiographical region 12 (Santa Rosalía). The North Clade had 2 subclades: the Vizcaíno Desert area and the region to the north (Fig. 3).
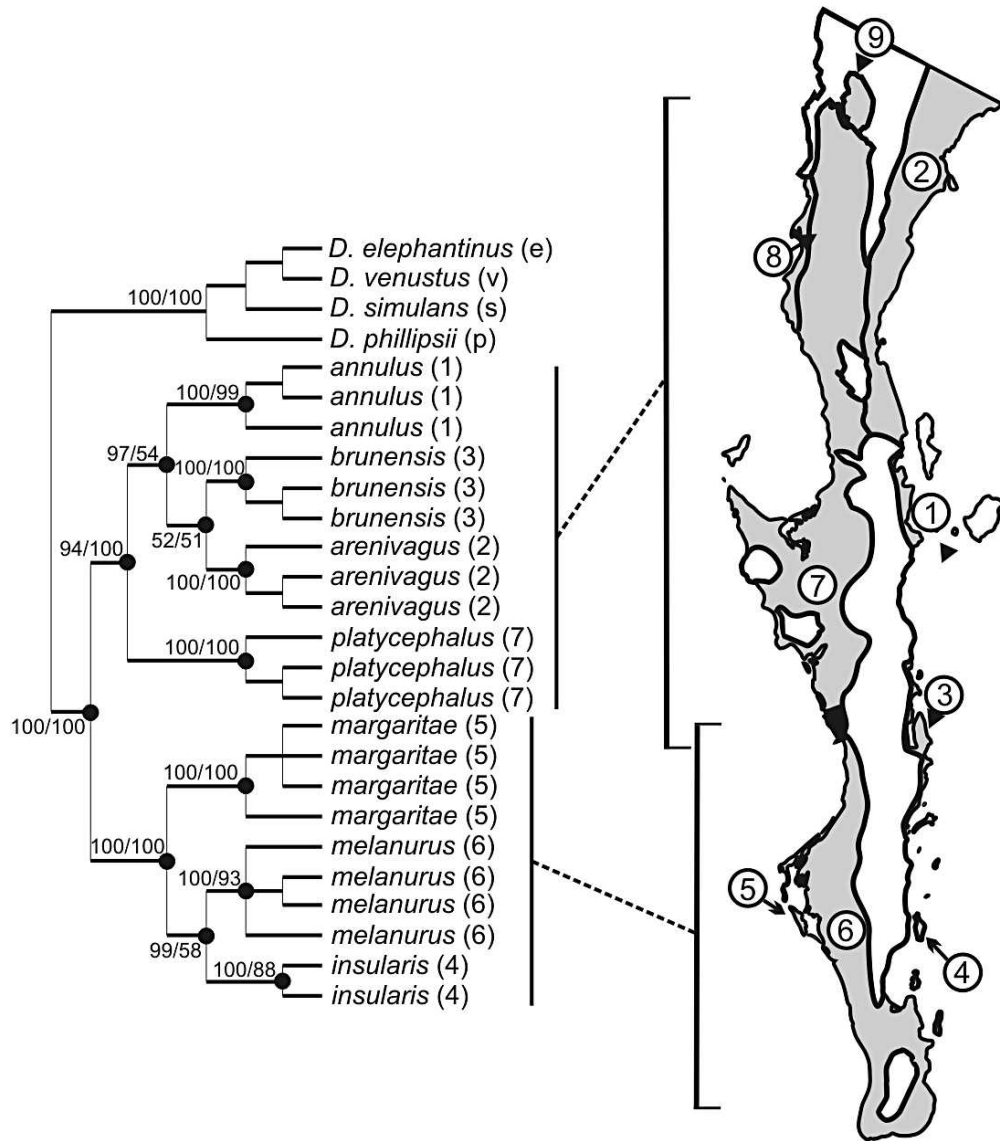
Fɪɢ. 3.—Topology of phylogenetic relationships among specimens of the *merriami* complex from the Baja California peninsula and surrounding islands based on the molecular data. On the left side of the figure are the analyses with concatenated 1,140 bp of the cytochrome *b* (*Cytb*) gene and 690 bp of the cytochrome *c* oxidase subunit III (*COIII*) gene. *Dipodomys simulans*, *D. phillipsii*, *D. venustus venustus*, and *D. v. elephantinus* were used as outgroups. The main topology was recovered from all the analyses and shows 2 monophyletic groups. One major clade contains specimens from the southern part of the peninsula including the island populations, and the 2nd includes the north-central region of the peninsula. Numbers at internal nodes are Bayesian posterior probabilities and bootstrap support of the Kimura 2-parameter model. The nodes with a black dot have 100% support in the maximum-parsimony and maximum-likelihood analyses. At the tip of each branch is the name and number of the subspecies shown in the map. 1) *D. m. annulus*, 2) *D. m. arenivagus*, 3) *D. m. brunensis*, 4) *D. m. insularis*, 5) *D. m. margaritae*, 6) *D. m. melanurus*, 7) *D. m. platycephalus*, 8) *D. m. quintinensis*, and 9) *D. m. trinidadensis*. Black area at the south end of the Vizcaíno Desert represents a zone of intergradation.

The maximum-likelihood analysis with the (GTR + I + G) evolution model produced only 1 tree (score = 6133; Fig. 3). Neighbor-joining analysis showed similar results to those obtained under the maximum-likelihood criteria. The specimens from San José and Margarita islands only had 1.07% and 0.97% of sequence divergence, respectively, from specimens from the mainland part of the southern Baja California peninsula. For the combined *Cytb* and *COIII* genes, there was only 1 haplotype found on San José Island and 3 on Margarita Island. The distance optimality criterion between the northern

and southern groups was 5.52% (Table 2). The values of haplotype diversity, nucleotide diversity, and mean number of pairwise differences obtained for *Cytb* for sampled populations from the southern Baja California peninsula and islands are shown in Table 1.

Morphological analysis.—The analysis of cranial morphology showed that the specimens from the northern part of the peninsula tended to be smaller than those from the south (Table 3), but no statistically significant differences were found between these 2 regions. However, some significant

TABLE 1.—Genetic parameters of the specimens from the different physiographic areas considered in the revision of the *Dipodomys merriami* complex: sample size (N_{ind}), numbers of haplotypes (N_{hap}), haplotype diversity, nucleotide diversity, and mean number of pairwise differences. Data are based on a 500-base-pair fragment of the cytochrome *b* gene. Regions are numbered consecutively as in the map (Fig. 1). Genetic data are not available for regions 2, 5, and 6.

Geographic area	N_{ind}	N_{hap}	Haplotype diversity	Mean no. pairwise differences	Nucleotide diversity
1 Mexicali—2 Laguna Salada	14	12	0.978 ± 0.034	7.065 ± 3.530	0.014 ± 0.007
3 Valle de la Trinidad	1	1	1.000 ± 0.000	0.000 ± 0.000	0.000 ± 0.000
4 San Felipe	2	1	0.000 ± 0.000	0.000 ± 0.000	0.000 ± 0.000
7 Cataviña	4	4	1.000 ± 0.176	12.833 ± 7.361	0.025 ± 0.017
8 Bahía de los Ángeles	16	11	0.933 ± 0.047	12.112 ± 5.673	0.024 ± 0.012
9 Vizcaíno Desert	24	18	0.974 ± 0.019	12.342 ± 5.806	0.024 ± 0.012
10 Bahía Tortugas	3	3	1.000 ± 0.272	12.666 ± 7.920	0.025 ± 0.019
11 San Juanico	12	10	0.969 ± 0.044	13.984 ± 6.755	0.027 ± 0.015
12 Santa Rosalía	3	3	1.000 ± 0.272	3.333 ± 2.323	0.006 ± 0.005
13 Hiray Plains	7	6	0.952 ± 0.095	16.523 ± 8.399	0.033 ± 0.019
14 Pacific Coast	4	2	0.500 ± 0.265	2.000 ± 1.405	0.004 ± 0.003
15 Magdalena Plains	11	9	0.945 ± 0.065	3.454 ± 1.908	0.006 ± 0.004
16 San José Island	4	1	0.000 ± 0.000	0.000 ± 0.000	0.000 ± 0.000
17 Margarita Island	9	2	0.222 ± 0.166	0.222 ± 0.288	0.000 ± 0.000
18 Cape Region	11	9	0.963 ± 0.051	3.236 ± 1.805	0.006 ± 0.004

differences ($P < 0.5$) were found between adjacent subregions throughout the peninsula (Figs. 4A–C).

The ANOVA for craniodental measurements revealed that all 9 measurements in the post hoc comparisons were significantly different in at least 1 comparison between 2 regions. However, the majority of these differences were not among populations in the same geographical area (Fig. 4A). The character that had the most significant differences among adjacent physiographical regions was maxillary breadth (ANOVA: $F = 23.508$, $d.f. = 17, 435$, $P = 0.0001$). Specimens from Bahía de los Ángeles (region 8) were significantly different ($P < 0.05$) in 6 of 9 characters from the Vizcaíno (region 9), and in 5 from Cataviña (region 7). Other regions showed only 1 or 2 characters that were significantly different (Fig. 4A); however, many adjacent regions did not have any characters that were significantly different between them.

Possible differentiation of populations living on Margarita and San José islands are of particular interest (Table 3). Table 4 summarizes the statistically significant differences

between these island populations and adjacent mainland regions, as well as differences between the 2 islands. They differed significantly ($P < 0.05$ or $P < 0.01$) from each other in 6 traits and from the intervening mainland by different cranial characters (Table 4).

The first 3 PCs for all of the craniodental measurements explained 71.1% of the variation (PC-I 47.7%, PC-II 13.7%, and PC-III 9.5%). PC-I did not show a consistent positive relation among its component characters, suggesting that it was not reflecting a size relationship among populations. The characters that explained the greatest amount of variation are: nasal length in PC-I, least width of supraoccipital in PC-II, and rostral width in PC-III. The 2nd of these traits had a comparatively high coefficient of variation when considered for the species as a whole (Baumgardner 1991; Baumgardner and Kennedy 1993; Lidicker 1960). Graphical analyses of PC-I versus PC-II, and PC-II versus PC-III (not shown) indicated an extensive overlap for all major regions and, hence, these analyses could not be used to distinguish among regions within the Baja California peninsula.

TABLE 2.—Genetic distances (%) obtained from the concatenation of the cytochrome *b* (*Cytb*, 1,140 bp) and cytochrome *c* oxidase subunit III (*COIII*, 690 bp) genes among (upper and lower matrices) and within (diagonal, in boldface type) proposed subspecies of *Dipodomys merriami* examined here. The upper-right matrix was generated using the GTR + I + G best model of evolution. Distances in the lower-left matrix and on the diagonal (boldface type) were generated using the Kimura-2-parameter model to allow comparison to traditional estimates of genetic distance in small mammals.

Subspecies	1	2	3	4	5	6	7	8
1) *annulus*	**0.20**	3.65	2.96	7.75	7.48	8.37	3.44	29.46
2) *arenivagus*	3.32	**1.35**	4.16	8.31	8.23	8.76	4.87	30.51
3) *brunensis*	2.72	3.70	**0.55**	7.22	7.49	8.13	3.92	30.35
4) *insularis*	6.59	6.84	6.05	**0.00**	0.95	1.07	7.15	29.42
5) *margaritae*	6.42	6.83	6.31	0.94	**0.07**	0.97	7.09	29.79
6) *melanurus*	7.04	7.17	6.74	1.03	0.94	**0.58**	7.95	29.38
7) *platycephalus*	3.10	4.21	3.47	6.01	5.99	6.59	**0.71**	29.36
8) Outgroups	15.97	16.25	16.14	16.29	16.13	15.88	15.73	**8.89**

TABLE 3.—Values of measured characters (mean $\pm$ *SD*; in mm) from the 2 subspecies in contact in the Baja California peninsula (*Dipodomys merriami platycephalus* and *D. m. melanurus*) and 2 island populations (*D. m. insularis* and *D. m. margaritae*). The acronyms for the traits are defined in the ''Materials and Methods''.

Trait	*D. m. platycephalus*	*D. m. melanurus*	*D. m. insularis*	*D. m. margaritae*
BLS	24.30 $\pm$ 0.70	24.90 $\pm$ 0.74	25.59 $\pm$ 0.76	24.47 $\pm$ 0.39
CL	35.78 $\pm$ 0.95	36.10 $\pm$ 0.94	36.26 $\pm$ 0.90	34.69 $\pm$ 0.62
NL	13.17 $\pm$ 0.54	13.21 $\pm$ 0.53	13.52 $\pm$ 0.49	12.97 $\pm$ 0.27
MxB	19.39 $\pm$ 0.74	20.07 $\pm$ 0.73	20.94 $\pm$ 0.57	19.39 $\pm$ 0.35
IB	12.74 $\pm$ 0.43	12.84 $\pm$ 0.47	13.00 $\pm$ 0.50	12.55 $\pm$ 0.32
CB	23.05 $\pm$ 0.60	23.08 $\pm$ 0.70	22.75 $\pm$ 0.62	21.58 $\pm$ 0.38
RW	3.01 $\pm$ 0.18	3.13 $\pm$ 0.23	3.56 $\pm$ 0.19	3.05 $\pm$ 0.14
ALMx	4.77 $\pm$ 0.29	4.88 $\pm$ 0.27	4.81 $\pm$ 0.17	5.03 $\pm$ 0.26
WS	1.37 $\pm$ 0.34	1.35 $\pm$ 0.35	1.33 $\pm$ 0.18	2.01 $\pm$ 0.18

The same analyses were performed separately on populations south of the Vizcaíno Desert (regions 11–18) and on populations from the Vizcaíno Desert and to the north (regions 1–10). The results were very similar to those for the peninsula as a whole. Even the 3 traits that explained the most variation were the same in each case. These principal component analysis results clearly showed that relationships among the parts of the skull are the same throughout the peninsula, and
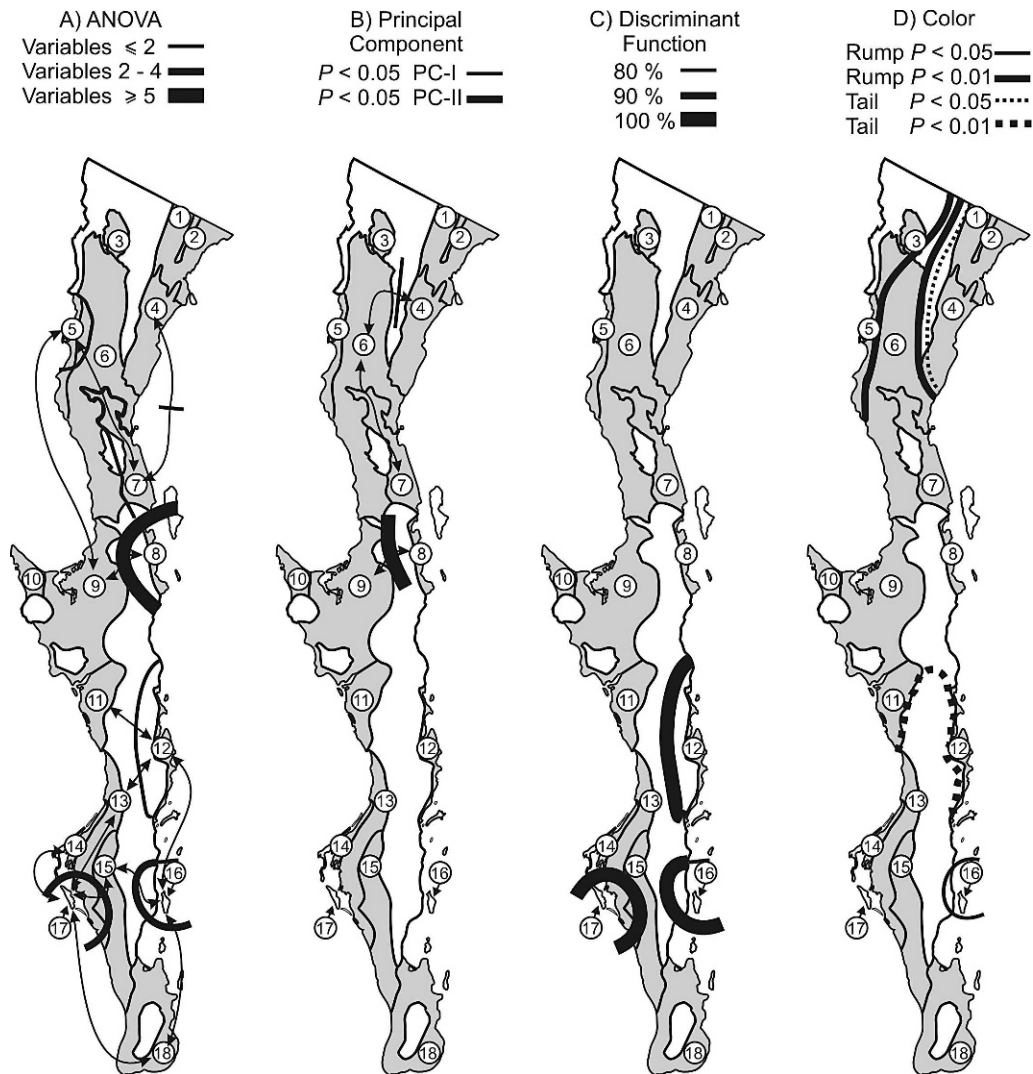

FIG. 4.—Summary of morphological analyses comparing the 18 physiographical regions (see Fig. 1): A) ANOVA for each of the 9 craniodental measurements; B) ANOVA of residuals of principal component I (PC-I) and PC-II of the principal component analysis for craniodental measurements; C) percentage of correct classifications according to the discriminant function analysis for all measurements; and D) ANOVA of the variation in pelage brightness.

TABLE 4.—Statistical comparisons of the craniodental measurements (in mm) between the 2 island populations and adjacent mainland areas made with Tukey's honestly significant difference test, using the unequal N (Spjotvoll/stoline—NS = not significant; * $P < 0.05$; ** $P < 0.01$). The numbers of the physiographic regions are given in parentheses; see Appendix I and Fig. 1. See ''Materials and Methods'' for definitions of acronyms of traits measured.

Trait		Region			
Margarita Island					
	Margarita Island (17)	Pacific Coast (13)	Hiray Plains (14)	Magdalena Plain (15)	Cape Region (18)
CB	21.57	20.40**	23.24**	23.50**	23.03**
CL	34.68	36.55**	35.97 NS	36.36*	35.85 NS
WS	2.00	1.49*	1.13**	1.22**	1.65 NS
San José Island					
	San José Island (16)	Santa Rosalía (12)	Magdalena Plain (15)	Cape Region (18)	Margarita Island (17)
BLS	25.59	24.25**	24.82*	22.77	24.47*
MxB	20.93	19.81**	20.37 NS	20.10*	19.38**
CB	22.75	22.78 NS	23.50*	23.08 NS	21.57*
RW	3.56	2.97**	3.16**	3.05**	3.05**
CL	36.25	35.72 NS	36.36 NS	36.38 NS	34.68*
WS	1.32	1.21 NS	1.22 NS	1.65 NS	2.00**

hence there was no evidence for any major developmental heterogeneities within the *D. merriami* complex inhabiting the peninsula.

The ANOVA of the residuals resulting from the principal component analysis for the Northern and Southern networks revealed that only the individuals from the Bahía de los Ángeles (region 8) were significantly ($P < 0.01$) bigger in relation to the specimens from other groups (Fig. 4B). No significant differences in size were found among the 8 groups located south of the Vizcaíno Desert (Fig. 4B).

The discriminant function analysis for all populations revealed that for the 3 populations from the central part of the Baja peninsula, specimens from Vizcaíno Desert had posterior probabilities as follows: 68.7% allocated to the Vizcaíno Desert (Fig. 4C, region 9), 25.0% to San Juanico (region 11), and 6.3% to Santa Rosalía (region 12). The
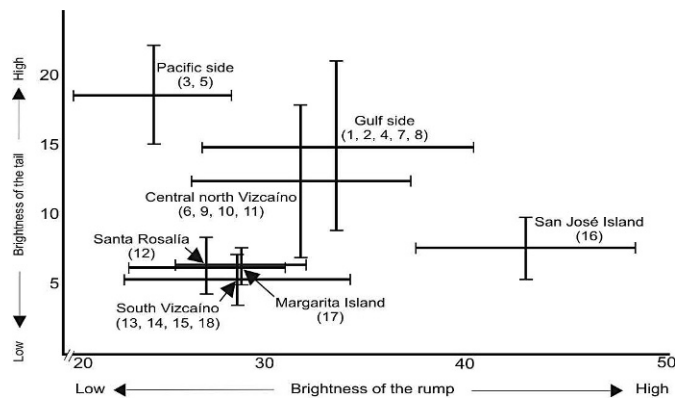

FIG. 5.—Principal component analysis of the brightness of the rump and tail coloration. The 18 regions are grouped into 7 representative groups. In parentheses are region numbers. Low brightness values are equivalent to dark coloration and high values to light colors.

specimens from San Juanico had a 50.0% posterior probability to be assigned to San Juanico, 40.0% to Vizcaíno Desert, and 10.0% to Santa Rosalía, and those from Santa Rosalía were assigned 95.5% to Santa Rosalía, 4.5% to Vizcaíno Desert, and none to San Juanico. In all the cases 50–95.5% of the specimens were correctly identified to their group.

The discriminant function analysis strongly discriminated between specimens from San José (region 16) and Margarita (region 17) islands in relation to the nearby mainland population. In both cases the allocation of posterior probabilities was 100% correct.

Color analysis.—The specimens with the darkest color were from the Cape (region 18) and from the northernmost extent of the range on the Pacific Coast (region 5), and the lightest were from the Mexicali–Laguna Salada–San Felipe regions (1, 2, and 4, respectively). A distinctive coloration characteristic is the dorsal tail stripe that ranged from black (Munsell chart score of 10YR 2/1) and broad in specimens from the Cape and northwestern coastal regions to pale brown (10YR 4/1) and narrow in the specimens from the northeastern deserts (Fig. 5). The brightness of the tail stripe can be used to distinguish between the populations south of the Vizcaíno Desert (dark tail) and those from the Vizcaíno Desert and other areas immediately to the north (light tail; Fig. 4D). However, individuals from south of San Ignacio Lagoon–San Juanico (region 11) had an intermediate coloration.

The brightness of the rump did not have a north–south axis of variation. However, the rump coloration can be used to distinguish the darker specimens from the Pacific side from the lighter specimens of the Gulf side of the peninsula (Figs. 2 and 5). The populations with light tails (north of Vizcaíno) can be divided into 3 groups in relation to the brightness of the rump: central north Vizcaíno, those with a distribution mostly inland from the Pacific Coast but on the western side of the

mountain range (region 3, 6, 9, 10, and 11), with a medium dark rump coloration; gulf side, the area that includes the coastal plains (regions 1, 2, 4, 7, and 8) on the east side of the mountain range with very light coloration; and Santa Rosalía (region 12), with a dark rump in combination with a moderately dark tail coloration. The specimens with dark tail stripes can be divided into 3 groups: the north Pacific Coast (region 5) with very dark and broad caudal stripes, San José Island (region 16) with relatively light rump coloration, and Margarita Island (region 17) plus the rest of the southern part of the peninsula (regions 13, 14, 15, and 18) with both dark rump and tail stripes.

DISCUSSION

Combining our molecular genetic data with new morphometric and pelage color analyses supports earlier studies of allozymic variation that considerable genetic structure exists within the populations of *D. merriami* inhabiting the Baja California peninsula. These results are commensurate with the topographic, edaphic, and climatic variation found in this region. In spite of this immense variation in available habitats, the species occurs over the entire peninsula and on 2 islands, except for the mountainous areas and the more mesic northwesternmost Pacific Coast (Fig. 3).

Examination of the molecular data corroborated a previous study (Riddle et al. 2000) that demonstrated 2 reciprocally monophyletic clades (Fig. 3): a Southern Clade that extends northward to the north end of the Hiray Plain on the western coast and to the La Paz isthmus and San José Island on the eastern coast, and a Northern Clade encompassing the rest of the distribution on the peninsula. There are 20 mutational steps in the DNA data that differentiate the Southern Clade and adjacent populations of the Northern Clade, although there is some intergradation in the vicinity of San Juanico at the southern extent of the Vizcaíno Desert (Fig. 2). Within the Southern Clade, there are 4 nested subclades: the mainland of the peninsula except for the Cape Region, the Cape Region itself, and 2 island groups (San José and Margarita; Fig. 2).

The Northern Clade is composed of 3 well-differentiated nested subclades (Fig. 2). A Central network extends along the west side of the mountain ranges from the southern end of Vizcaíno Desert north to the latitude of Cataviña. A 2nd network (Coastal) extends along a narrow coastal zone from Loreto to Santa Rosalía and from El Barril to Bahía de los Ángeles. Finally, a Northern network includes the rest of the distribution to the north.

Combining the phylogenetic and nested clade analyses shows that the Southern Clade is coincident with the Southern network. The Central, Coastal, and Northern networks are all contained within the Northern Clade.

A smaller amount of differentiation within the Central network exists between the western and eastern sides of the distribution, and between the 2 nested subclades of the Coastal network (Fig. 2). We are unsure about the relationship of populations inhabiting the narrow coastal zone along the Pacific Coast (El Rosario north to the vicinity of San Quintín)

because we were unable to obtain molecular data from individuals from that region (5).

The percent difference in the molecular data across the 2 monophyletic clades revealed by the phylogenetic analysis is 6.07% for *Cytb* concatenated with *COIII*. This degree of difference is in the range sometimes considered to represent the species level of differentiation (Bradley and Baker 2001). However, the AMOVA shows more variation within the clades (94.6% of the genetic variation) than between them. Moreover, there is some genetic mixing between the 2 clades and the morphological difference across the boundary is relatively small. We therefore conclude that species-level differentiation is not present, and all populations in the peninsula should be considered 1 species, *Dipodomys merriami*. However, the clear phylogenetic break suggests that isolation between these 2 major clades is quite ancient, although continuing contact has prevented attainment of species level. This important genetic division was 1st recognized by Riddle et al. (2000) and then corroborated by Alexander and Riddle (2005), who reported a similar genetic distance for the *COIII* gene of 4.1%. Moreover, this discontinuity corresponds to the border between 2 physiographical regions (11 and 13) of Cuanalo et al. (1989), as defined by Goldman and Moore (1946) and Álvarez and De LaChica (1974).

Differentiation of the 2 island forms from the mainland population appears to be relatively recent. The Margarita Island population was 1.0% different from the adjacent mainland for *Cytb*, and 1.2% for *COIII*. Individuals from San José Island are 1.2% different for *Cytb* and 0.6% for *COIII*. On the other hand, these 2 island forms show strong morphological and color differentiation from the mainland (Table 3; Álvarez 1960; Best 1992; Best and Janecek 1992; Best and Thomas 1991; Lidicker 1960). Combining data sets, we conclude that these island populations should be viewed as well-differentiated subspecies: *Dipodomys merriami insularis* for San José Island and *D. m. margaritae* for Margarita Island. The mainland portion of the Southern Clade should remain as *D. m. melanurus*. The relatively weak mtDNA differentiation suggests that the morphological and color differentiation has occurred quite rapidly in these subspecies. Of the 3, *D. m. insularis* exhibits traits that are relatively unspecialized for open desert conditions, which is a pleisiomorphic feature for the species as a whole (Lidicker 1960). *D. m. insularis* has the lowest combined specialization score based on 3 indices of specialization among all forms of the *D. merriami* complex of subspecies (Lidicker 1960; Table 2). *Dipodomys m. margaritae* also is quite ''primitive'' in this regard, ranking 3rd out of 19 taxa for being the least specialized. We therefore surmise that rapid morphological change toward increasing arid adaptations within the Southern Clade involved mainly *D. m. melanurus*. In support of this, we note that *D. m. melanurus* shows haplotype structure suggesting sequential expansion of its haplotype diversity. Moreover, we find that the 2 island populations differ significantly from each other in 6 cranial traits, and each differs from *D. m. melanurus* in 3 different cranial features (Table 4).

Enlarged auditory bullae relative to the rest of the skull (known to enhance hearing and possibly balance) and elongated hind feet (an adaptation for enhanced saltatory abilities) are considered to be evidence of derived (more specialized for aridity) morphology. Moreover, hot air temperatures have relatively poor sound-transmitting properties (Knudsen 1935). In kangaroo rats, these features are found to be associated with the most open and relatively arid habitats (Lidicker 1960). We speculate that the retention of relatively unspecialized morphologies in the 2 island forms is related to the lack of mammalian predators on these islands, and, in the case of San José Island, also to the relatively dense shrubby cover in which they live. Both islands have other potential predators on kangaroo rats such as hawks, owls, and snakes, but perhaps it is the lack of predators such as foxes that actively hunt on the ground and chase prey that is the critical factor. Such predators inevitably make sounds as they move about, and locate prey moving in the openings among the vegetation.

We suggest that it is the absence of mammalian predation on the 2 islands that is the primary factor leading to a lack of selective pressures needed to evolve the derived morphology. In support of this argument, we point out that the subspecies *arenivagus* lives in the most open and arid habitats on the peninsula, and correspondingly has the most derived morphology.

Our results with the 2 island taxa support our argument that taxonomic analyses at the species and subspecies levels should ideally be based on data sets that are sensitive to different time dimensions of history. Morphologically, the forms *insularis* and *margaritae* are quite distinct from mainland subspecies, and this level of differentiation explains why some earlier workers viewed the island populations as being distinct species from *D. merriami*. On the other hand, examination of the molecular data clearly implies a fairly recent separation of the island forms from the mainland. For both the morphological and molecular conclusions to be true, the observed morphological differentiation (Table 4) must have evolved quite rapidly. We surmise that *D. m. melanurus* responded to selection pressures centered on mammalian predation, and that this response was likely facilitated by gene flow from the north bringing in genes for the more derived morphologies.

Based on calculated sea-level changes, Lidicker (1960) suggested that San José Island may have been isolated about 12,000 years ago. The isolation of Margarita Island is more difficult to estimate because of ongoing tectonic activity along the west coast. Currently, however, the island is <1 km from a neighboring island (which itself is <1 km from the mainland), and Magdalena Bay is relatively shallow, all of which suggest that isolation is fairly recent.

An interesting question, therefore, is why the observed morphological diversity in this species has been so rapid. Many studies have shown that pelage color matching to background conditions can proceed quickly (Hoekstra 2006; Hoekstra et al. 2005; Krupa and Geluso 2000; Mullen and Hoekstra 2008; Steiner et al. 2007). Almost all the peninsular mainland populations share the same level of specialization with respect to cranial and pedal indices (Lidicker 1960; Table 2). Only 2 northern peninsular subspecies are different in this respect: *arenivagus*, which is distinctly more derived, and *quintinensis*, which is moderately less specialized. This implies that most of the mainland forms have responded morphologically to similar ecological contexts in spite of underlying deep genetic structuring revealed by the molecular data.

We cannot be confident that the island forms have retained their less-specialized features as pleisiomorphic traits or secondarily evolved these traits in response to the relatively predator-free conditions on their islands. On both islands, only 10% or less of the island areas contain suitable habitat for kangaroo rats, and so effective population sizes might be quite small. The population on San José Island does have a reduced mean coefficient of variation for cranial measurements compared to mainland populations (2.03 versus 3.16). In contrast, kangaroo rats on Tiburón Island, a much larger island also in the Sea of Cortez, show a mean coefficient (3.21) that is equivalent to those of mainland populations (Lidicker 1960; Table 1). San José Island individuals also have reduced allozymic variation when compared to their mainland relatives in terms of number of alleles per locus, percent of heterozygous loci, and percent of polymorphic loci (Best and Janecek 1992). Comparable genetic data are not available for *margaritae*, but it remains plausible that these island populations have been few in number and depauperate in genetic variation for a long time.

Our results for the Northern Clade generally support the subspecific arrangement of Lidicker (1960). The Central subclade corresponds to the subspecies *D. m. platycephalus*. The Northern subclade consists of the subspecies *D. m. arenivagus* and *D. m. trinidadensis*. The latter is a closely related derivative of *arenivagus* and differences are mainly morphological, particularly in color. It occurs in the high-elevation valleys of Trinidad and San Rafael on the west side of the Sierra Juárez. It now seems doubtful that it extends farther north into southern San Diego County, California, as reported in Lidicker (1960). These morphologically similar populations in California are probably independently derived from *D. m. arenivagus* responding similarly to similar environments. *D. m. trinidadensis* connects with *D. m. arenivagus* through San Matías Pass separating the Sierra Juárez from the Sierra San Pedro Mártir. We were not able to reevaluate the status of the Pacific Coast subspecies *D. m. quintinensis*. The San Quintín Plain, in which it occurs, has been completely converted to agricultural production, and we were not able to obtain new material for this analysis. Lidicker (1960) reported that *D. m. quintinensis* intergrades with *D. m. platycephalus* south and east of El Rosario and presumably is derived from that form. We recommend continuing recognition of this subspecies in the hopes that additional information on its characteristics and population status will be forthcoming. Its conservation status should be investigated urgently.

Somewhat surprisingly we found that the 2 disjunct populations making up the Coastal nested clade are sister taxa. They are quite distinct from each other morphologically and in coloration (Lidicker 1960). We affirm their status as *D.*

m. annulus for the more northerly population and *D. m. brunensis* for the southern population. It now appears that both were derived from *D. m. arenivagus* through dispersal down the east side of the peninsula along the narrow coastal band of suitable habitat. Subsequent sea-level rises likely led to their current isolation from each other.

This investigation has resulted in significantly increasing our phylogenetic and biogeographic understanding of the patterns of genetic structuring found in this widespread kangaroo rat species inhabiting the Baja California peninsula. At the same time, the new information has supplemented rather than contradicted our understanding based on earlier morphological analyses. In some cases examination of the genetic data indicated a deeper differentiation than reported in other studies, and in other situations the reverse was true. Overall, our results support the importance of using multiple data sets in phylogenetic analyses, because various types of data reflect different time frames of evolutionary change. Our understanding of the evolutionary history of *D. merriami* is thereby enhanced by this expanded historical context.

RESUMEN

La rata canguro *Dipodomys merriami* ocurre ampliamente por la península de Baja California, habitando todas las zonas áridas y arenosas de baja altitud. Su distribución incluye áreas con diversas características de clima, suelo y vegetación, incluyendo 2 islas. En esta región se reconocen 11 taxa para el complejo *merriami* desde hace casi 50 años, siendo aun válidos hasta la fecha. Las 2 formas isleñas fueron descritas como especies diferentes; no obstante, han sido tratadas de diversas maneras por posteriores autores. En esta investiga-ción se utilizó un análisis genético de 2 genes mitocondriales, el citocromo *b* (*Cytb*) y citocromo *c* oxidasa subunidad III (*COIII*), para estudiar los patrones de estructura genética en esta especie a lo largo de la península. Complementamos la información morfométrica y de coloración del pelaje pre-viamente reportada con nuevos datos obtenidos por nosotros, los cuales integramos a la información filogenética. Por último, analizamos nuestros resultados con los arreglos taxonómicos actuales para las especies y subespecies. Nuestro análisis filogenético incluyó 1,140 pb del gen *Cytb* y 690 pb del *COIII* usando los procedimientos de máxima parsimonia, máxima probabilidad e inferencia Bayesiana. Se realizó un análisis de clados anidados donde se revelaron en el nivel más alto 2 clados monofiléticos separados por 20 pasos mutacio-nales. Hay un Clado Sur que se extiende hasta el norte del Desierto del Vizcaíno en el oeste y a la Isla San José por el este, y un Clado Norte que incluye el resto de las poblaciones con distribución más norteña. En un nivel menos profundo, el Clado Sur contiene 4 subclados, incluyendo las poblaciones de las islas San José y Margarita, mientras que el Clado Norte está conformado por 3 sublcados. Los análisis morfométricos y de coloración del pelaje, adicionales a los genéticos, soportan el arreglo en una sola especie de los 11 taxa previamente reconocidos, correspondiendo a *Dipodomys merriami*, con un mejor entendimiento de cómo se relacionan las subespecies entre sí.

LITERATURE CITED

ALEXANDER, L. F., AND B. R. RIDDLE. 2005. Phylogenetics of the New World rodent family Heteromyidae. Journal of Mammalogy 86:366–379.

ÁLVAREZ, T. 1960. Sinopsis de las especies Mexicanas del género *Dipodomys*. Revista de la Sociedad Mexicana de Historia Natural 21:391–424.

ÁLVAREZ, T., AND F. DE LACHICA. 1974. Zoogeografía de los vertebrados de México. Pp. 217–302 in El escenario geográfico, recursos naturales (J. L. Lorenzo, ed.). Instituto Nacional de Antropología e Historia, Mexico City, Mexico.

ÁLVAREZ-CASTAÑEDA, S. T., C. A. SALINAS-ZAVALA, AND F. DE LACHICA. 1995. Análisis biogeográfico del noroeste de México con énfasis en la variación climática y mastozoológica. Acta Zoológica Mexicana, nueva serie 66:59–86.

BAKER, R. J., AND R. D. BRADLEY. 2006. Speciation in mammals and the genetic species concept. Journal of Mammalogy 87:643–662.

BAUMGARDNER, G. D. 1991. Individual nongeographic variation and character relationships in kangaroo rats (genus *Dipodomys*). Texas Journal of Science 43:345–356.

BAUMGARDNER, G. D., AND M. L. KENNEDY. 1993. Morphometric variation in kangaroo rats (genus *Dipodomys*) and its relationship to selected abiotic variables. Journal of Mammalogy 74:69–85.

BEST, T. L. 1992. *Dipodomys margaritae*. Mammalian Species 400:1–3.

BEST, T. L., AND L. L. JANECEK. 1992. Allozymic and morphologic variation among *Dipodomys insularis*, *Dipodomys nitratoides* and two populations of *Dipodomys merriami*. Southwestern Naturalist 37:1–8.

BEST, T. L., AND H. H. THOMAS. 1991. *Dipodomys insularis*. Mammalian Species 374:1–3.

BRADLEY, R. D., AND R. J. BAKER. 2001. A test of genetic species concept: cytochrome-*b* sequence and mammals. Journal of Mammalogy 84:960–973.

CLEMENT, M., D. POSADA, AND K. CRANDALL. 2000. TCS: a computer program to estimate gene genealogies. Molecular Ecology 9:1657–1660.

CUANALO, H., E. OJEDA, A. SANTOS, AND C. A. ORTIZ. 1989. Provincias y subregiones terrestres de México. Colegio de Postgraduados, Chapingo, México.

ESPINOZA-GAYOSSO, C. V., AND S. T. ÁLVAREZ-CASTAÑEDA. 2006. Status of *Dipodomys insularis*, an endemic species of San José Island, Gulf of California, Mexico. Journal of Mammalogy 87:677–682.

GANNON, W. L., R. S. SIKES, AND THE ANIMAL CARE AND USE COMMITTEE OF THE AMERICAN SOCIETY OF MAMMALOGISTS. 2007. Guidelines of the American Society of Mammalogists for the use of wild mammals in research. Journal of Mammalogy 88:809–823.

GOLDMAN, E. A., AND R. T. MOORE. 1946. Biotic provinces of Mexico. Journal of Mammalogy 26:347–360.

HALL, R. E. 1981. The mammals of North America. John Wiley and Sons, Inc., New York.

HOEKSTRA, H. E. 2006. Genetics, development and evolution of adaptive pigmentation in vertebrates. Heredity 97:222–234.

HOEKSTRA, H. E., J. G. KRENZ, AND M. W. NACHMAN. 2005. Local adaptation in the rock pocket mouse (*Chaetodipus intermedius*): natural selection and phylogenetic history of populations. Heredity 94:217–228.

KNUDSEN, V. O. 1935. Atmospheric acoustics and the weather. Scientific Monthly 40:485–486.

KRUPA, J. J., AND K. N. GELUSO. 2000. Matching the color of excavated soil: cryptic coloration in the plains pocket gopher (*Geomys bursarius*). Journal of Mammalogy 81:86–96.

LIDICKER, W. Z., JR. 1960. An analysis of intraspecific variation in the kangaroo rat *Dipodomys merriami*. University of California Publications in Zoology 67:125–218.

LIDICKER, W. Z., JR. 1962. The nature of subspecies boundaries in a desert rodent and its implications for subspecies taxonomy. Systematic Zoology 11:160–171.

MERRIAM, C. H. 1907. Description of ten new kangaroo rats. Proceedings of the Biological Society of Washington 20: 75–79.

MULLEN, L. M., AND H. E. HOEKSTRA. 2008. Natural selection along an environmental gradient: a classic cline in mouse pigmentation. Evolution 62:1555–1570.

MUNSELL COLOR CO. 1975. Munsell soil color charts. Munsell Color Company, Baltimore, Maryland.

NYLANDER, J. A. A. 2004. MrModeltest v2.2. Program distributed by the author, Evolutionary Biology Center, Uppsala University, Uppsala, Sweden.

PANCHAL, M. 2007. The automation of nested clade phylogeographic analysis. Bioinformatics 23:509–510.

PANCHAL, M., AND M. A. BEAUMONT. 2007. The automation and evaluation of nested clade phylogeographic analysis. Evolution 61:1466–1480.

PATTON, J. L., AND S. T. ÁLVAREZ-CASTAÑEDA. 1999. Family Heteromyidae. Pp. 351–443 in Mamíferos del noroeste Mexicano (S. T. Álvarez-Castañeda and J. L. Patton, eds.). Centro de Investigaciones Biológicas del Noroeste, S.C., La Paz, Mexico.

PATTON, J. L. 2005. Heteromyidae. Pp. 844–858 in Mammals species of the world: a taxonomic and geographic reference. 3rd ed. (D. E. Wilson and D. M. Reeder, eds.). Johns Hopkins University Press, Baltimore, Maryland.

PATTON, J. L., D. G. HUCKABY, AND S. T. ÁLVAREZ-CASTAÑEDA. 2007. The systematic and evolutionary history of woodrats of the *Neotoma lepida* complex. University of California Publications in Zoology 135:1–411.

POSADA, D., K. A. CRANDALL, AND A. R. TEMPLETON. 2000. GeoDis: a rogram for the cladistic nested analysis of the geographical distribution of genetic haplotypes. Molecular Ecology 9:487–488.

RIDDLE, B. R. 1995. Molecular biogeography in the pocket mice (*Perognathus* and *Chaetodipus*) and grasshopper mice (*Onychomys*): the late Cenozoic development of a North American aridlands rodent guild. Journal of Mammalogy 76:283–301.

RIDDLE, B. R., D. J. HAFNER, L. F. ALEXANDER, AND J. R. JAEGER. 2000. Cryptic vicariance in the historical assembly of a Baja California peninsular desert biota. Proceedings of the National Academy of Sciences 97:14438–14443.

RONQUIST, F., AND J. P. HUELSENBECK. 2003. MrBayes3: Bayesian phylogenetic inference under mixed models. Bioinformatics 19:1572–1574.

SCHNEIDER, S., D. ROESSLI, AND L. EXCOFFIER. 2000. Arlequ: a software for population genetics data analysis. Ver. 2.001. Genetics and Biometry Lab, Department of Anthropology, University of Geneva, Geneva, Switzerland.

STEINER, C. C., J. N. WEBER, AND H. E. HOEKSTRA. 2007. Adaptive variation in beach mice caused by two interacting pigmentation genes. PLoS Biology 5:1880–1889.

SWOFFORD, D. L. 2000. PAUP*: phylogenetic analysis using parsimony (*and other methods), version 4.0b10. Sinauer Associates, Inc., Publishers, Sunderland, Massachusetts.

TAVARÉ, S. 1986. Some probabilistic and statistical problems in the analysis of DNA sequences. Lectures on Mathematics in the Life Sciences 17:57–86.

TEMPLETON, A. R., E. BOERWINKLE, AND C. F. SING. 1987. A cladistic analysis of phenotypic associations with haplotypes inferred from restriction endonuclease mapping. I. Basic theory and an analysis of alcohol dehydrogenase activity in *Drosophila*. Genetics 117:343–351.

TEMPLETON, A. R., K. A. CRANDALL, AND C. F. SING. 1992. A cladistic analysis of phenotypic associations with haplotypes inferred from restriction endonuclease mapping and DNA sequence data. III. Cladogram estimation. Genetics 132:619–633.

TEMPLETON, A. R., AND C. F. SING. 1993. A cladistic analysis of phenotypic associations with haplotypes inferred from restriction endonuclease mapping. IV. Nested analysis with cladogram uncertainty and recombination. Genetics 134:659–669.

WILLIAMS, D. F., H. H. GENOWAYS, AND J. K. BRAUN. 1993. Taxonomy. Pp. 38–196 in Biology of the Heteromyidae (H. H. Genoways and J. H. Brown, eds.). Special Publication 10, The American Society of Mammalogists.

APPENDIX I

Locality designation for each geographic area (listed numerically as in map in Fig. 1); and sample sizes for morphologic ($_{morph}$), coloration ($_{color}$), and genetic ($_{DNA}$) analyses. Museum catalogue numbers are provided for the specimens examined. Collection acronyms are as follows: American Museum of Natural History (AMNH); Centro de Investigaciones Biológicas del Noroeste (CIB); Colección Nacional de Mamíferos, Universidad Nacional Autónoma de México (CNMA); Museum of Vertebrate Zoology, University of California (MVZ); San Diego Natural History Museum (SDNHM); University of California, Los Angeles (UCLA); and United States National Museum of Natural History (USNM).

1. Mexicali (n = 16$_{morph}$, 8$_{color}$, 2$_{DNA}$).—10 km E San Luís Río Colorado (CIB 4394); 23 km S, 64 km E San Luís Río Colorado (CIB 8238); Imperial Canal, 11 miles E Mexicali (MVZ 32240); 10 W Pilot Knob, 1 mile S United States–Mexico border (MVZ 39302, 39303); Alamo River, 20 miles SW Pilot Knob (MVZ 39277–39290, 39304).

2. Laguna Salada (n = 23$_{morph}$, 41$_{color}$, 12$_{DNA}$).—13 miles N El Mayor (MVZ 37821, 37824); Cerro ''El Centenario'' 3.2 km N, 22 km W Mexicali (CIB 10484–10486); Cerro Centinela, 13 miles WSW Mexicali (MVZ 111586–111588); 18.5 km S, 35 km W Mexicali (CIB 10488); 21 km S, 31.5 km W Mexicali (CIB 10489–10493); Olivar, 46 km S, 21 km W Mexicali (CIB 7114–7116); 47 km S, 37 km W Mexicali (CIB 7131); E side Cocopah Mts.,

21 miles SSE Mexicali (MVZ 111589, 111590); 78.6 km S, 14.7 km W Mexicali (CIB 10496, 10497); Ejido El Saldaña, 83 km S, 5 km W Mexicali (CIB 7331, 7134–7139); 89.7 km S, 11.5 km W Mexicali (CIB 10487, 10498); Colorado River, 20 miles S Pilot Knob (MVZ 39292–39301); Los Palmas Canyon, W side Laguna Salada (MVZ 39305–39310, 39312–39314); 31 miles N and 7 miles W San Felipe (MVZ 124213, 124215, 124225–124227.

3. Valle de la Trinidad (n = 51$_{morph}$, 41$_{color}$, 1$_{DNA}$).—Sangre de Cristo (SDNHM 6052–6054, 6069, 6070, 6077, 6099, 6100, 6112, 6142, 6163, 6368, 6372–6374, 6413–6415); Rancho Sangre de Cristo, 31.5 miles E Ensenada (MVZ 148113–148131); Valle de La Trinidad (SDNHM 6307, 6524, 6578, 11523–11530, 11532, 11533, 11535, 11536, 11567–11570, 11594, 11635, 11636, 11679, 11680); El Valle de La Trinidad (MVZ 38080); 6 km S and 17 km E Valle de La Trinidad (MVZ 153984); 9.2 miles E and 6.6 miles S Colonia Cárdenas (MVZ 148103–148112); 8 miles S, 10 miles E Valle de la Trinidad (CIB 3209–3217); 2 km N, 9 km E Ojos Negros (CIB 7332); S San Mateo Pass (SDNHM 11759–11764, 11853–11855).

4. San Felipe (n = 45$_{morph}$, 20$_{color}$, 2$_{DNA}$).—1 km W San Felipe (CIB 3159, 3160); San Felipe (CNMA 8743, 8744; MVZ 37795–37798, 37801, 37802, 37804, 37805, 37807, 37811, 37815, 37816, 37820; SDNHM 5117, 5151, 5163, 5232, 8608–8615, 8621–8623, 8625, 8626, 8628, 8659–8662, 8735, 8740, 8741, 8747, 8751–8753); 3 miles SSW San Felipe (MVZ 124207, 124208, 124211, 124217, 124219); 8 km S, 10 km E San Felipe (CIB 7140–7145); mouth of El Cajon Canyon, E base of San Pedro Martir Mts. (MVZ 37825–37828).

5. San Quintín (n = 46$_{morph}$, 31$_{color}$).—Arroyo Nuevo York, 15 miles S Misión Santo Domingo (MVZ 36241–36250); San Quintín (MVZ 49880–49891, 49893); N end San Quintin Plain (CNMA 162; SDNHM 4937–4939, 4960–4962); Santo Domingo (MVZ 36235–36240, 36251; SDNHM 4668, 4679, 4680, 4684, 4693); Agua Chiquita, 4 miles E San Quintin (MVZ 35702, 35703); 1 km E San Quintín (CIB 4034); 10 miles E San Quintin (SDNHM 18576, 18587–18589, 18604, 18617, 18619, 18621).

6. Santa Catarina (n = 17$_{morph}$, 6$_{color}$).—8 km N Santa Catarina (SDNHM 15856, 15858, 15877, 15878, 15900, 15901); 7 km N Santa Catarina (SDNHM 4270, 4272–4275, 8498–8503); Santa Catarina, 40 km W Cataviña (CIB 3740); ''La Ramona,'' 7 km N, 37 km W Cataviña (CIB 3734–3739).

7. Cataviña (n = 96$_{morph}$, 24$_{color}$, 4$_{DNA}$).—12.5 miles S by road El Marmol (MVZ 111591–111594); Distrito Norte, 5 miles S El Marmol (MVZ 97550); La Bocana del Cañón de Santa María (MVZ 49955–49959); 1 km W Cataviña (CIB 3175); Cataviña (MVZ 49874, 49911–49927, 49929–49948, 49951–49954); Puerto de Calamajue (MVZ 49961–49970); San Agustín (MVZ 49898–49904, 49909, 49910; SDNHM 8137, 8138, 8160, 8180, 8185); 26 km N, 14 km W Cataviña (CIB 2536–2539); 11 km N, 8.5 km W Cataviña (CIB 2541, 2543–2546); 25 miles N Punta Prieta (CNMA 8438, 8440; SDNHM 8437, 8439, 8444, 8471, 8472); 24 miles NW Punta Prieta (MVZ 111595–111597); 23 km N, 21 km W Bahía San Luis Gonzaga (CIB 3168–3174).

8. Bahía de los Ángeles (n = 24$_{morph}$, 35$_{color}$, 16$_{DNA}$).—15 km N, 20 km E Bahía de los Ángeles (CIB 4020); 4 km N, 20 km W Bahía de los Ángeles (CIB 4012, 4014, 4016, 4017); 2 km N, 15 km W Bahía de los Ángeles (CIB 9151–9155); Bahía de los Ángeles (CIB 3151, 3152, 3154–3157); Las Flores (SDNHM 15731, 15734, 15735, 15739, 15740, 15744, 15747); Las Flores, 14 km S Bahía de los Ángeles (CIB 9156–9160); Valle Las Flores (CIB 3723, 3724); 19 km S, 28 km E Bahía de Los Ángeles (CIB 7093–7099); San Francisquito Bay (AMNH 31973–31975); 7 miles W San Francisquito Bay (SDNHM 15608, 15629, 15644, 15646, 15669, 15670);

3 km S, 8 km W Punta San Francisquito (CIB 3725); 7 km N, 14 km W El Progreso (CIB 7194–7198); El Progreso (CIB 3726–3728); El Barril (SDNHM 15491, 15493, 15511, 15523, 15530, 15550, 15564, 15573); 40 km N, 40 km E El Arco (CIB 9161–9164); 36 km N, 40 km E El Arco (CIB 9167, 9168).

9. Vizcaíno Desert (n = 16$_{morph}$, 24$_{color}$, 24$_{DNA}$).—12 km N, 24 km E Nuevo Rosarito (CIB 10532); 5.2 km N, 22 km W Nuevo Rosarito (CIB 10535); 4 km N, 2 km W Nuevo Rosarito (CIB 2554, 4031–4033); 8 km S, 13.2 km W Nuevo Rosarito (CIB 10537); 4 km N, 29.5 km W Punta Prieta (CIB 10531); Punta Prieta (CNMA 8773; MVZ 49971; SDNHM 6771, 6772, 6778, 6779, 6787, 6788, 6793–6795, 6812); 40 km N, 40 km E El Arco (CIB 9161–9164); 36 km N, 40 km E El Arco (CIB 9165–9168); 19 km N, 12.5 km W El Arco (CIB 9169, 9170, 9174); El Arco (CIB 9175); Calmallí (CIB 9171–9173; CNMA 6985; MVZ 49972–49975); 19.2 km N, 24.5 km E Guerrero Negro (CIB 10570, 10571); 3 km N, 15.5 km E Guerrero Negro (CIB 9573, 9574); 8.7 km S, 9.2 km E Guerreo Negro (CIB 9581–9584); 46 km S, 26.2 km E Guerrero Negro (CIB 10549, 10554); 48 km S, 23.7 km E Guerrero Negro (CIB 10560, 10563); Corral de Berrendos, 61 km S, 5 km W Guerrero Negro (CIB 7214–7216); Belisario Dominguez, 24.7 km S, 49.7 km W Vizcaíno (CIB 10578, 10579, 10581, 10582); 13 km S, 30 km W Vízcaino (CIB 9179, 9182, 9183); 2 km N, 500 m E San José de Castro (CIB 10575); 1.5 km N, 5.2 km E San José de Castro (CIB 10576); 4 km S, 3 km E San José de Castro (CIB 9580); 20 km N, 26.3 km E Estero La Bocana (CIB 9650–9652); 38 km N, 19 km E Punta Abreojos (CIB 9587); 1 km N, 43 km W San Ignacio (CIB 9176); 6 km S, 3 km W San Ignacio (CIB 7297, 7299, 7308, 7310).

10. Bahía Tortugas (n = 24$_{morph}$, 10$_{color}$, 3$_{DNA}$).—Malarrimo, 10 km N, 20 km E Bahía Tortugas (CIB 7227, 7229, 7230); Bahía Tortugas (CIB 10556, 10565–10567, 10572; MVZ 49905–49908; UCLA 17896, 17897); Bahía Asunción (CIB 9586, 9610, 9611, 9613, 9625–9627, 9629–9632, 9635, 9636).

11. San Juanico (n = 11$_{morph}$, 15$_{color}$, 12$_{DNA}$).—40 km N, 5 km E San Juanico (CIB 9661–9672); 4 km S, 24 km E San Juanico (CIB 9669–9673); 43 km S, 21 km W San Ignacio (CIB 9186); 70 km S, 18 km W San Ignacio (CIB 7316, 7317); 76 km S San Ignacio (CIB 9655, 9658, 9659); Batequi, 33 km N, 60 km W La Purísima (CIB 7321, 7323, 7324, 7326, 7327).

12. Santa Rosalía (n = 25$_{morph}$, 12$_{color}$, 3$_{DNA}$).—10 km N, 14 km W Santa Rosalía (CIB 2555); 10 miles W Santa Rosalia (SDNHM 6913, 6914, 6918, 6919); 10 miles SW Santa Rosalia (CNMA 6920); 25 km S, 7 km E Santa Rosalía (CIB 3732, 3733); Mulege (MVZ 111632); Bahía Concepción, 13 miles SE Mulege (MVZ 111633–111636); S end Bahía Concepción (SDNHM 14831–14833, 14835–14838, 14845, 14846, 14854–14858); Santa Rosalillita, SE end Bahía de Concepción (MVZ 111637); 10.3 km S, 12.7 km W Mulegé (CIB 10015, 10016); 31 km S, 30 km W Mulegé (CIB 1165, 2838); 17.9 km N, 7.8 km W Loreto (CIB 11216); 13.8 km S, 1.3 km W Loreto (CIB 11215); 17.9 km N, 7.8 km W Loreto (CIB 11216).

13. Hiray Plains (n = 16$_{morph}$, 23$_{color}$, 7$_{DNA}$).—W end Llano de Yirais (MVZ 111638–111640); 24.3 miles SE (by road) El Refugio (MVZ 111641–111643, 111646); 9 miles S El Refugio (SDNHM 14645–14647, 14666, 14667); Distrito Sur, near El Refugio, 24.3 miles SE by road (MVZ 97552, 111641–111643, 111645, 111646, 111648, 111649); 18.1 km N, 24 km E La Purísima (CIB 10017, 10018); 3 km S, 5 km W La Purísima (CIB 9678, 9681); 5 km S, 7 km W San Miguel de Comondú (CIB 9689, 9690); Los Laureles, 16.5 km S, 7.5 km W San Isidro (CIB 7686–7690).

14. Pacific Coast (n = 15$_{morph}$, 9$_{color}$, 4$_{DNA}$).—5 km N, 16 km E Puerto López Mateos (CIB 6494, 6495); 1 km S, 6 km E Puerto

López Mateos (CIB 6496–6499); San Jorge (MVZ 111650–111653; SDNHM 14750); 3 km E Puerto San Carlos (CIB 6500–6503); 1 km S, 4 km E Puerto San Carlos (CIB 6504, 6505).

15. Magdalena Plains (n = 33$_{morph}$, 28$_{color}$, 11$_{DNA}$).—Santo Domingo (MVZ 49979, 49980; SDNHM 14688, 14706, 14737, 14738); 16 km N, 24 km E Ciudad Constitución (CIB 10021); Ciudad Constitución (CIB 7147, 7149, 7151–7154); 11.9 km S, 13.6 km W Villa Morelos (CIB 11218); Santa Rita (CIB 7162, 7163, 7165, 7166, 7169); 2.6 km S, 31.5 km W Santa Rita (CIB 11220); 6.2 km S, 9.5 km E Santa Rita (CIB 11221); Matancita (MVZ 49976–49978); Brisamar, 25 km W La Paz (CIB 487, 492, 8050–8054, 8056); El Comitán, 17.5 km W La Paz (CIB 4946, 4948); La Paz (SDNHM 14506, 14507, 14509, 14616, 14618, 14635, 14637, 14638); 1 miles S La Paz (MVZ 42979–42984); 2 miles SW La Paz (MVZ 42967–42977, 42987).

16. San Jose Island (n = 15$_{morph}$, 16$_{color}$, 4$_{DNA}$).—San Jose Island (UCLA 18000, 50183); Isla San José (CIB 11000–11003); SW end San Jose Island (MVZ 42988–42999).

17. Margarita Island (n = 10$_{morph}$, 10$_{color}$, 9$_{DNA}$).—Santa Margarita Island (UCLA 17906, 17907, 17924, 17930; USNM 146057, 146061, 146062; Isla Margarita (CIB 5128, 6059, 6065); Playa Occidental, Isla Margarita (CIB 6059–6064); 2 km W Puerto Cortés, Isla Margarita (CIB 5127, 5128); Agua Amarga, 4 km S Puerto Cortés, Isla Margarita (CIB 6065, 6066).

18. Cape Region (n = 27$_{morph}$, 20$_{color}$, 11$_{DNA}$).—2.5 km W Ensenada de Muertos (CIB 5884); Ensenada de Muertos (CIB 5874–5877, 5885–5887); Bahía de Muertos (UCLA 50688); 3 km N El Sargento (CIB 5878, 5879, 5881, 5882); 11.5 km N, 6.6 km E El Triunfo (CIB 11227); 4 km NE Santiago (CIB 8231–8235); Todos Santos (MVZ 42963–42966); Agua Caliente (MVZ 43002, 43003, 43007–43012, 43015); Buena Vista (SDNHM 14675, 14677–14679); San José del Cabo (MVZ 43000, 43001, 111654; SDNHM 14535, 14549, 14550, 14561–14563); Cape San Lucas (CNMA 90816).

Appendix II

Haplotype designation (H*n*), as is shown in Fig. 2, and locality for representative specimens for each subspecies. In parentheses are the decimal degrees of latitude and longitude followed by the number of museum repository of the Centro de Investigaciones Biológicas, La Paz, Baja California Sur, Mexico (CIB) or Las Vegas Tissue collection (LVT). Sequences with AY initials were obtained from GenBank (accession number), and those with EU were generated for this study.

Dipodomys merriami annulus.—Region 8: H41, EU661018 *Cytb*, 36 km N, 40 km E El Arco (28.358, −112.988, 9167); H46, EU661019 *Cytb*, 36 km N, 40 km E El Arco (28.358, −112.988, 9168); H47, EU660980 *Cytb*, 7 km N, 14 km W El Progreso (28.404, −113.135, 7198); H50, EU660977 *Cytb*, 40 km N, 40 km E El Arco (28.062, −112.993, 9164); H54, EU660978 *Cytb*, 7 km N, 14 km W El Progreso (28.404, −113.135, 7195); H55, EU661066 *Cytb*; EU660976 *COIII* (CIB 7096), 7 km N, 14 km W El Progreso (28.404, −113.135, 7196); 19 km S, 28 km E Bahía de Los Ángeles (28.780, −113.199, 7096); H56, EU667416 *Cytb*, 40 km N, 40 km E El Arco (28.062, −112.993, 9161–9163); 7 km N, 14 km W El Progreso (28.404, −113.135, 7197); H57, EU661064 *Cytb*, EU660974 *COIII*, 19 km S, 28 km E Bahía de Los Ángeles (28.780, −113.199, 7093, 7095); H58, EU661065 *Cytb*, EU660975 *COIII*, 19 km S, 28 km E Bahía de Los Ángeles (28.780, −113.199, 7094); H59, EU661020 *Cytb*, 19 km S, 28 km E Bahía de Los Ángeles (28.780, −113.199, 7097); H60, EU661049 *Cytb*, Malarrimo, 10 km N, 20 km E Bahía Tortugas (27.783, −114.697, 7227);

H74, EU667412 *Cytb*, 7 km N, 14 km W El Progreso (28.404, −113.135, 7194).

Dipodomys merriami arenivagus.—Region 1: H66, EU660981 *Cytb*, 10 km E San Luis Río Colorado (32.421, −114.579, 4394); H67, EU660986 *Cytb*, 23 km S, 64 km E San Luis Río Colorado (32.261, −114.069, 8238); H70, EU661023 *Cytb*, Olivar, 46 km S, 21 km W Mexicali (32.233, −115.695, 7114–7116); H72, EU667413 *Cytb*, Ejido El Saldaña, 83 km S, 5 km W Mexicali (31.917, −115.383, 7331); H77, EU660984 *Cytb*, Ejido El Saldaña, 83 km S, 5 km W Mexicali (31.917, −115.383, 7138); H81, EU660983 *Cytb*, Ejido El Saldaña, 83 km S, 5 km W Mexicali (31.917, −115.383, 7134). Region 2: H68, EU661067 *Cytb*, EU660965 *COIII*, 18.5 km S, 35 km W Mexicali (32.458, −115.803, 10488); EU660966 *Cytb*, EU661068 *COIII*, 21 km S, 31.5 km W Mexicali (32.427, −115.770, 10493); H75, EU660985 *Cytb*, 47 km S, 37 km W Mexicali (32.222, −115.865, 7131, 7133); H78, EU660987 *Cytb*, 78.6 km S, 14.7 km W Mexicali (31.938, −115.631, 10496, 10487); H79, EU661024-*Cytb*, 21 km S, 31.5 km W Mexicali (32.427, −115.770, 10492); H80, EU660988 *Cytb*, 89.7 km S, 11.5 km W Mexicali (31.837, −115.566, 10498). Region 4: H69, EU661069 *Cytb*, 1 km W San Felipe (31.023, −114.842, 3159, 3160); EU660967 *COIII*, 5.2 km N, 16 km W San Felipe (31.066, −115.017, 12062). Region 7: H38, EU661044 *Cytb*, 23 km N, 21 km W Bahía San Luis Gonzaga (29.958, −114.503, 3171); H51, EU661045 *Cytb*, 23 km N, 21 km W Bahía San Luis Gonzaga (29.958, −114.503, 3174); H52, EU661043 *Cytb*, 23 km N, 21 km W Bahía San Luis Gonzaga (29.958, −114.503, 3170); H73, EU661022 *Cytb*, 1 km W Cataviña (29.733, −114.733, 3175).

Dipodomys merriami brunensis.—Region 12: H61, EU661026 *Cytb*, 10.3 km S 12 .7 km W Mulegé (26.804, −112.109, 10016); H62, EU661025 *Cytb*, 10.3 km S, 12 .7 km W Mulegé (26.804, −112.109, 10015); H63, EU661058 *Cytb*, EU660963 *COIII*, 17.9 km N, 7.8 km W Loreto (26.160, −111.428, 11216).

Dipodomys merriami insularis.—Region 17: H17, AY926371 *Cytb*, AY926438 *COIII*, Isla San José (24.950, −110.651, 2103, 2107, 2111, 2112, LVT 2043).

Dipodomys merriami margaritae.—Region 16: H11, EU661059 *Cytb*, EU660970 *COIII*, Playa Occidental, Isla Margarita (24.407, −111.823, 6059–6061, 6063, 6064); Agua Amarga, 4 km S Puerto Cortés, Isla Margarita (24.439, −111.826, 6065, 6066); 2 km W Puerto Cortés, Isla Margarita (24.475, −111.846, 5128); H12, AY926370 *Cytb*, AY926437 *COIII*, Isla Margarita (24.475, −111.846, LVT 2042).

Dipodomys merriami melanurus.—Region 11: H4, EU661007 *Cytb*, Batequi, 33 km N, 60 km W La Purísima (26.438, −112.765, 7323). Region 13: H1, EU660999 *Cytb*, 5 km S, 7 km W San Miguel de Comondú (25.982, −111.922, 9690); H2, EU660997 *Cytb*, 5 km S, 7 km W San Miguel de Comondú (25.982, −111.922, 9689); H6, EU660998 *Cytb*, 3 km S, 5 km W La Purísima (26.178, −112.112, 9681); H7, EU660996 *Cytb*, 3 km S, 5 km W La Purísima (26.178, −112.112, 9678); H64, EU661057 *Cytb*, EU660964 *COIII*, 18.1 km N, 24 km E La Purísima (26.359, −111.853, 10017, 10018, 10019). Region 14: H5, EU661031 *Cytb*, 1 km S, 6 km E Puerto López Mateos (25.185, −112.059, 6496); H23, EU661032 *Cytb*, 1 km S, 4 km E Puerto San Carlos (24.774, −112.079, 6504); San Jorge (25.726, −112.074, 7160); H28, EU661063 *Cytb*, EU660973 *COIII*, 4 km E, 1 km S Pto. San Carlos (24.781, −112.061, 7157). Region 15: H4, EU661029 *Cytb*, El Comitán, 17.5 km W La Paz (24.138, −110.467, 4946); 6.2 km S, 9.5 km E Santa Rita (24.534, −111.370, 11221); Ciudad Constitución (25.039, −111.652, 7151); 16 km N, 24 km E, Ciudad Constitución (25.182, −111.416, 10021); H23,

EU661038 *Cytb*, Brisamar, 25 km W La Paz (24.149, −110.543, 8053); 1 km S, 4 km E Puerto San Carlos (24.774, −112.078, 6504, 7157); San Jorge (25.726, −112.074, 7160); H24, EU661030 *Cytb*, El Comitán, 17.5 km W La Paz (24.138, −110.467, 4948); H25, EU661027 *Cytb*, Brisamar, 25 km W La Paz (24.149, −110.543, 487); H26, EU661062 *Cytb*, EU660972 *COIII*, 2.6 km S, 31.5 km W Santa Rita (24.570, −111.775, 11220); H27, EU661033 *Cytb*, Ciudad Constitución (25.039, −111.652, 7149); H29, EU661039 *Cytb*, Brisamar, 25 km W La Paz (24.149, −110.543, 8054); H30, EU661028 *Cytb*, Brisamar, 25 km W La Paz (24.149, −110.543, 492); H31, EU661061 *Cytb*, EU660971 *COIII*, 11.9 km S, 13.6 km W Villa Morelos (24.821, −111.766, 11218). Region 18: H3, EU660991 *Cytb*, Ensenada de Muertos (23.999, −109.827, 5877); H14, EU660992 *Cytb*, Ensenada de Muertos (23.999, −109.827, 5876); H15, EU660994 *Cytb*, 4 km NE Santiago (23.502, −109.758, 8235); Ensenada de Muertos (23.999, −109.827, 5885); H16, EU661000 *Cytb*, 11.5 km N, 6.6 km E El Triunfo (23.913, −109.979, 11227); H18, EU660995 *Cytb*, 4 km NE Santiago (23.502, −109.758, 8232–8234); H20, EU661040 *Cytb*, 4 km NE Santiago (23.502, −109.758, 8231); H21, EU660990 *Cytb*, Ensenada de Muertos (23.999, −109.827, 5875); H22, EU660993 *Cytb*, 2.5 km W Ensenada de Muertos (23.999, −109.851, 5884).

Dipodomys merriami platycephalus.—Region 9: H6, EU661011 *Cytb*, 20 km N, 26.3 km E Estero La Bocana (26.993, −113.021, 9651); H9, EU661009 *Cytb*, 4 km S, 3 km E San José de Castro (27.510, −114.458, 9580); Calmallí (28.106, −113.429, 9171); H10, EU661002 *Cytb*, 6 km S, 3 km W San Ignacio (24.244, −112.922, 7308); H13, EU661003 *Cytb*, 6 km S, 3 km W San Ignacio (24.244, −112.922, 7310); H34, EU661055 *Cytb*, 48 km S, 23.7 km E Guerrero Negro (27.543, −113.859, 10563); Malarrimo, 10 km N, 20 km E Bahía Tortugas (27.783, −114.697, 7230); H35, EU661017 *Cytb*, 8 km S, 13.2 km W Nuevo Rosarito (28.560, −114.147, 10537); H37, EU661056 *Cytb*, 1.5 km N, 5.2 km E San José de Castro (27.547, −114.422, 10576); H38, EU661016 *Cytb*, 5.2 km N,

22 km W Nuevo Rosarito (28.678, −114.243, 10535); H39, EU661053 *Cytb*, 19 km N, 12.5 km W El Arco (28.210, −113.519, 9170, 9174); H40, EU661048 *Cytb*, Corral de Berrendos, 61 km S, 5 km W Guerrero Negro (27.402, −114.019, 7216); 6 km S, 3 km W San Ignacio (24.244, −112.922, 7299); 19 km N, 12.5 km W El Arco (28.210, −113.519, 9169); H42, EU661070 *Cytb*, EU660968 *COIII*, 2 km N, 500 m E San José de Castro (27.564, −114.469, 10575); H44, EU661047 *Cytb*, Corral de Berrendos, 61 km S, 5 km W Guerrero Negro (27.402, −114.019, 7215); 20 km N, 26.3 km E Estero La Bocana (26.993, −113.021, 9650); H46, EU661010 *Cytb*, El Arco (28.014, −113.365, 9175); H48, EU667414 *Cytb*, 20 km N, 26.3 km E Estero La Bocana (26.993, −113.021, 9652); H49, EU661001 *Cytb*, 6 km S, 3 km W San Ignacio (24.244, −112.922, 7297); H50, EU661046 *Cytb*, Corral de Berrendos, 61 km S, 5 km W Guerrero Negro (27.402, −114.019, 7214); 1 km N, 43 km W San Ignacio (27.301, −113.322, 9176); H53, EU661015 *Cytb*, 4 km N, 29.5 km W Punta Prieta (28.962, −114.508, 10531). Region 10: H34, EU661071 *Cytb*, EU660969 *COIII*, Malarrimo, 10 km N, 20 km E Bahía Tortugas (27.783, −114.697, 7226, 7230); H42, EU661050 *Cytb*, Malarrimo 10 km N, 20 km E Bahía Tortugas (27.783, −114.697, 7229). Region 11: H6, EU661008 *Cytb*, Batequi, 33 km N, 60 km W La Purísima (26.438, −112.765, 7327); 76 km S San Ignacio (26.639, −112.894, 9655); H8, EU661054 *Cytb*, 40 km N, 5 km E San Juanico (26.483, −112.687, 9664); H32, EU661013 *Cytb*, 76 km S San Ignacio (26.639, −112.894, 9658); H33, EU661005 *Cytb*, 70 km S, 18 km W San Ignacio (26.629, −113.031, 7317); H36, EU661004 *Cytb*, 70 km S, 18 km W San Ignacio (26.629, −113.031, 7316); H39, EU661006 *Cytb*, Batequi, 33 km N, 60 km W La Purísima (26.438, −112.765, 7321); H40, EU661014 *Cytb*, 76 km S San Ignacio (26.639, −112.894, 9659); 43 km S, 21 km W San Ignacio (26.901, −113.098, 9186); H43, EU667415 *Cytb*, Batequi, 33 km N, 60 km W La Purísima (26.438, −112.765, 7326); H45, EU661052 *Cytb*, Batequi, 33 km N, 60 km W La Purísima (26.438, −112.765, 7324).